CHAPTER 3.

TWO-DIMENSIONAL NON-LINEAR MODEL OF THE ANISOTROPIC TRANSIENT HEAT CONDUCTION IN WOOD

Summary

This chapter discusses the development of a two-dimensional heat conduction model using the theoretical values of the thermal conductivity derived in the previous chapter. The model was set up based on the energy conservation law and solved by the Finite Difference method. Program was written in the *Mathematica* software. Good visualization for the results from the *Mathematica* output can aid the scientific research and industry operation.

The model predicted transient temperature distribution in the two transverse directions of wood with the specified thermal conductivities in the two directions. A simulation was run on an ideal situation with the perfect wood structure (ring orientation on the cross section) for the modeling, in order to investigate the anisotropic material property affects on the heat transportation in wood and the boundary effects on internal heat transfer. Time series analysis for simulation results inferred reliability of the theoretical values for the radial and tangential thermal conductivities derived in the previous chapter.

Validation tests for the 2D model were done on the three species in the previous chapter -- southern yellow pine, Scots pine and soft maple. Modification of the thermal conductivity in the two practical directions for ordinary wood blocks was made before running the 2D model. Comparison of the model output with the testing results demonstrated good predictions by the model solved in this chapter. Sensitivity of the parameters used in the 2D model were studied to examine their relative importance and contributions to the heat transfer in wood.

3.1 Introduction

The previous chapter dealt with thermal conductivity in the two transverse directions. Thermal conductivity plays an important role in wood heat transport processes. Heat transfer in the two transverse directions is usually of interest to the wood industry because most of the heat transfer applications for wood are in the transverse direction, such as lumber drying in kilns and log heating in veneer and plywood mills. Knowledge of the transient temperature profile in wood is very helpful to the operation and simulation.

With knowledge of the thermal conductivity changes with structure, temperature and moisture content from the previous chapter, modeling of the heat transfer in wood becomes more dependable. After more than fifty years of heat and mass transfer modeling in wood, it has been found (Kamke & Vanek 1994, Hukka 1997) that the agreement between the model and experiments does not depend on the complexity of the theory but rather on the number of parameters employed and the effort put into the evaluation of their numerical values. Most of the previous modeling used the parameters found in the literature based on experimental results. Different parameters and values used in the models may cause extreme differences in the model output. Using the evaluated theoretical values of the parameters for the model, such as the theoretical thermal conductivity values derived in the previous chapter, should give the consistency and completeness for the models because theoretical values of these parameters can be interpolated and extrapolated in a wide range.

Wood is a hygroscopic and porous medium. Heat transfer in wood may occur by several modes: 1).Conduction in the solid cell wall substance and liquid or gaseous water in the cell lumen; 2).Convection in the cell lumen; 3).Radiation from wall substance when the temperature in wood is high enough. Convection and radiation play very small parts in the wood heat transportation process, so the model developed in this chapter is only for the conduction process. Wood is an anisotropic material. Heat conduction in the three anatomical directions of wood (radial, tangential and longitudinal) will be different if the thermal conductivities are different. This chapter is to model the transient heat conduction process in the two transverse directions based on the theoretical thermal conductivity values obtained from the previous chapter. The two dimensional modeling is a non-linear model due to the temperature-dependence of the two transverse thermal conductivities. The transient temperature profiles can be easily visualized in the powerful *Mathematica* software.

Simulation using the 2D model was run on southern yellow pint for an ideal geometric structure on the cross section of the wood block, which was assumed to be subjected to a heating process. The anisotropic material structure effects on the heat transportation process were analyzed.

Validation tests for the pure 2D heat conduction model were performed on the sample blocks from the three species chosen for modeling in this study. In practical sample blocks and lumber used in the industry, the ideal geometric structure defined in the model -- the perfect radial and tangential directions (defined in the anatomical structure) coincident with the two transverse directions in the testing blocks, -- is very rare. Therefore some modifications of the thermal conductivity values used in the model's two directions were made before comparing the model output and the experimental results. Sensitivity studies on some parameters used in the model were performed to gain the insight of the relative importance of these parameters and their effects on the temperature profiles.

The main purpose for this chapter is to model the 2D heat conduction during the wood heating process by use of theoretically derived thermal conductivity parameters from the previous chapter, and to examine the anisotropic material properties effects on the transfer process and the boundary condition effects on the internal heat transfer process.

3.2 Background

There is a long history of heat and mass transfer studies in wood science. Models of heat and mass transfer have been developed from empirical models (Rosen 1987) to theoretical models (Luikov 1975, Chen & Pei 1989, Bonneau 1993 and Pang et al. 1994), from one dimensional models (Plumb et al. 1985, Stanish et al. 1986, Sutherland et al. 1992, Liu et al. 1994 and Pang et al. 1994) to two or three dimensional models (Perre et al. 1993, Perre et al. 1999, Perre &Turner 1999, Ferguson & Turner 1994, and Pang 1996) . Review of the modeling research has been done by several researchers (Borries 1989, Parrouffe & Mujumdar 1988, Salin 1991 and Kamke & Vanek 1992).

Most of the heat and mass transfer models are based on energy conservation and mass conservation laws and momentum equations. Values of physical properties for solutions are either found from the literature or estimated by the curve-fitting process for model output with one set of experimental results. Bramhall (1977) studied the processes involved in wood drying and distinguished it as: 1). Heat transfer through the boundary layer; 2). Heat conduction in wood; 3). Mass flow of moisture by capillarity; 4). Evaporation from the wood surface; and 6). Transfer of latent heat with diffusing and evaporating molecules. He modeled the heat conduction by using the Fourier's equation:

$$\frac{\partial H}{\partial t} = K \frac{\partial^2 T}{\partial x^2}$$

Equa (3. 1)

For mass transfer he used the simple diffusion equation. All the parameters involved in the model are either obtained directly from the literature or calculated from empirical equations given in the literature. For thermal conductivity used in his heat conduction model, he used the equation given by Stamm (1964) as a function of density, moisture content and void space in wood. The one-dimensional model developed by Stanish, et al. (1986) assumed wood is a homogenous material. The model is for flow in the transverse direction. It is a relative complete one dimensional model for heat and mass transfer by including a set of fundamental transport equations (mass conservation, energy conservation) coupled with a thermodynamic equilibrium equation. The model successfully predicted experimental drying behavior of wood. The heat and mass transfer properties required in the model were studied and obtained from the steam table and physical property handbook. Some of these properties have significant dependencies with temperature and

moisture content. In the conclusion, they pointed out that knowledge of the material property variation is the key for model improvement. Vogel (1989) developed a one-dimensional model for unsteady-state mass diffusion and heat conduction in wood. The mass diffusion coefficient was estimated from Siau's (1984) geometrical model and analogous electrical resistance circuit in the transverse direction. Another one-dimensional wood drying model for scotch pine (*Pinus sylvestris*) was developed by Ranta-Maunus (1992, 1994). His model included the consideration of property differences between heartwood and sapwood. Later he developed this one-dimensional model into a two dimensional model with the assumption of equal transport properties in the radial and tangential directions. Bonneau & Puiggali (1993) studied the details for the affects of different properties from heartwood and sapwood on the two dimensional drying model outputs. A two driving-force model, external and inter-region heat transfer potential is used to compare a homogeneous and a heterogeneous approach to the drying of a pinewood board. The main difference between the two theoretical descriptions is adding a specific boundary condition for the inter-region (or interface) between the sapwood and heartwood for the heterogeneous model. Transport properties were separated from sapwood and heartwood for the heterogeneous model. In the homogeneous model, the effective transport coefficients were obtained by a homogenization procedure. In the comparison of the two models and comparison with the experimental results, the heterogeneous approach provides a good description (profiles and drying kinetic curve) of a heartwood-sapwood drying problem, however, the homogeneous model will generally provide the results fast and correctly in terms of the macroscopic description of the drying kinetics. The heterogeneities considered in this model are only limited to the macroscopic level, i.e. the heartwood and sapwood proportion in a board. Only a few studies have been devoted to this type of analysis for the modeling. Salin (1990) developed an interesting analysis of the influence of heartwood-sapwood proportion on drying and due-to-drying degradation processes. Pang (1994) studied the different mechanisms for the moisture movement in heartwood and sapwood. He postulated that in the drying of heartwood liquid flow does not occur within the board due to the aspirated state of the pits. In the case of the wetter sapwood where the pits are not aspirated initially, liquid flow maintains an evaporative plane just below the surface. Based on this mechanism difference and properties difference in the heartwood and sapwood, one-dimensional (Pang 1994) and two-dimensional (Pang 1996) models were solved by him and compared with the experimental results. The two dimensional model was for the moisture movement and heat transfer in thickness and width directions. The model is based on the physiological properties of both green and drying wood with heartwood being distinguished from

sapwood. The same thermal conductivity values used for the two directions in the model were calculated from the equation given by Stanish et al. (1986) as a function of moisture content.

Perre et al. (1999) proposed a 2-D model for a straightforward and efficient simulation of drying for a porous material that treated wood as a strongly anisotropic medium. The model simulation was run on both anisotropic (wood) and isotropic (light concrete) porous media. His model was solved differently from other researchers by a semi-analytical method using enough physical assumptions. The anisotropy was only reflected in the model when the permeability was of interest, but for the heat transfer within the medium, anisotropy is assumed to occur only in the thickness direction for simplifying the governing equations. The model was calibrated by using experimental results, with the primary fitted parameters being the averaged physical properties of the product. Then the two simulations run by the model for the softwood heartwood and sapwood drying process obtained good agreement with the experimental results. Later, Perre & Turner (1999) developed this 2D TransPore version model into a 3-D model. It is the first drying model that deals with a comprehensive set of macroscopic equations in three spatial dimensions. Simulations were run for softwood high temperature and low temperature convective drying process. The simulations prove that only three spatial dimensions are able to capture the effect of the width of the medium in the case of high temperature drying. For strongly anisotropic (especially in the 3 dimensions) medium as wood, all the physical properties in the three directions were distinguished. Only the theoretical model was studied in their research. Validation tests for the 3D model were not available.

Steinhagen (1985) used a temperature method and an enthalpy method to solve the transient temperature profiles for frozen logs subjected to axisymmetric heating. The conventional equation for non-linear heat conduction is as:

$$\frac{1}{r}[\frac{\partial}{\partial r}(kr\frac{\partial T}{\partial r})] = \rho c\frac{\partial T}{\partial t}$$

Equa (3. 2)

The thermal properties used in the computation were varied with position and temperature, and changed discontinuously with the phase. Good agreement was obtained between the computed temperature profiles and the experimental data obtained from heating logs.

Khattabi & Steinhagen (1992) developed a theoretical solution for two-dimensional heating of logs. The numerical solution is based on the enthalpy method and orthogonal cylinder

system. The thermal conductivities in the two-dimensional heat model were referenced to the longitudinal and radial direction. They were evaluated based on the temperature, moisture content and specific gravity using Steinhagen & Lee (1988)'s equation:

$$k_r = (1380 + 19MC + 2.2T_{avg} + 0.11MC \cdot T_{avg}) \times (0.105 + 2.03SG) \times 10^{-4}$$

Equa (3. 3)

The longitudinal thermal conductivity value used in their model was assumed to be twice the calculated radial values. To evaluate this theoretical model, a general accepted analytical solution using constant thermal properties was compared with the model predictions. Only 10% discrepancy was found between the two solutions. Later (Khattabi & Steinhagen 1994) a 3D transient heat conduction model was developed for a rectangular piece of wood and also an orthotropic wooden cylinder. The finite-difference technique was applied to solve this non-linear problem. No validation tests were performed for the theoretical 3D model.

Puiggali & Quintard (1992) demonstrated that drying phenomena for wood are very complex in nature due to its heterogeneous nature at the different scales of observation. For the heterogeneous medium as wood, with naturally built up growth rings, the elementary transport mechanisms can be studied by one-phase flow (Quintard & Whitaker 1987) and two-phase flow (Quintard & Whitaker 1988). For simplification, some studies (Plumb et al. 1985, Stanish et al. 1986, Michel et al. 1987 and Perre 1987) treated wood as a homogeneous medium. They showed that modeling a homogeneous capillary porous body would, under certain conditions, successfully represent the internal processes. But the actual data and numerical predictions often show some significant discrepancies for moisture content near the FSP. One possible explanation is the effect of heterogeneities from one growth ring to the other. Puiggali & Quintard (1992) gave an illustration for scaling of the observation for wood drying modeling (Figure 3.1).

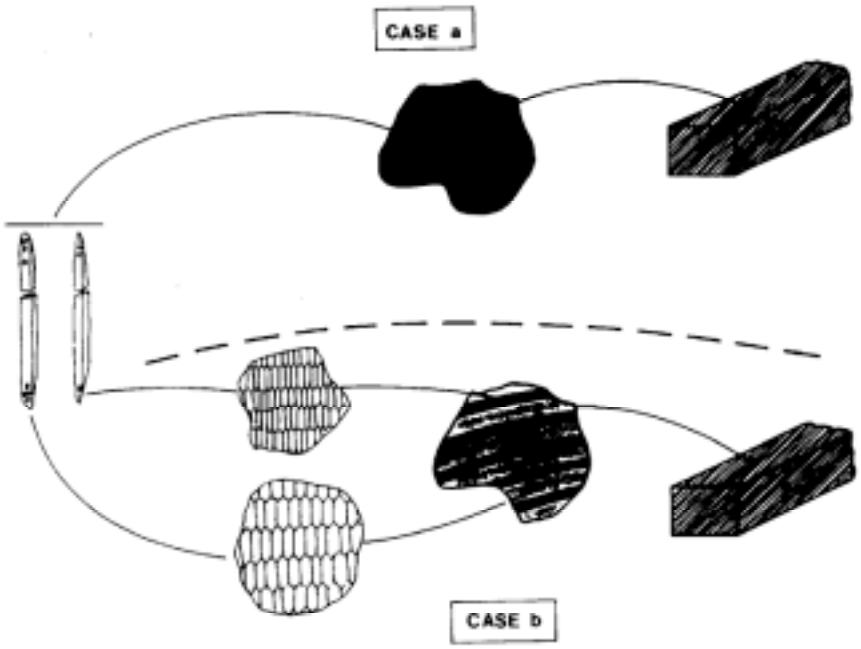

Figure 3. 1 Scaling of a wood drying process. Case a). for homogeneous, Case b). for heterogeneous. (Puiggali & Quintard, 1992)

3.3 Model development

Heat and mass transfer in wood during drying or heating usually occurs in the transverse direction because the length (longitudinal direction) of wood is usually much longer than the thickness and width in the transverse direction. The two dimensional transient heat model will be set up for the transverse (width and thickness) heat conduction based on the energy conservation law and using the material properties (thermal conductivity) derived from the previous chapter. The anisotropic effect on heat transport in the radial and tangential directions by different transport properties will be examined. Non-linearity for the model comes from the temperature dependence of the thermal conductivities.

3.3.1 Model assumptions

Since the model developed in this study is to investigate the different heat transfer property effects on the heat transport in wood, only heat transfer was modeled without mass transfer coupled with it. To solve a mathematical model for a physical problem, no matter numerically or semi-analytically, there are always some assumptions based on understanding of the materials and phenomenon for simplifying the problem.

The assumptions for modeling the two dimensional anisotropic heat transfer process in wood are as follows:

A. Heat conduction is the major transfer mechanism for wood subjected to an ordinary heating process, such as drying. Radiation can be ignored when the temperature is not high enough. Convective heat transfer in wood was also neglected in the model due to the very low velocity of air or vapor movements in the cell lumen.

B. The model is two dimensional for the wood thickness and width, neglecting the heat transfer in the longitudinal direction;

C. The thermal conductivity in radial (k_r) and tangential (k_t) directions are functions of moisture content and temperature but assumed to be constant with respect to the spatial coordinates.

D. No chemical reaction occurs within wood. Therefore no heat generation inside the wood during the heating process is considered in this model;

E. Surface radiation is neglected;

F. The boundary conditions are assumed to be the same on the four sides of the wooden board with the convective heat transfer boundary.

3.3.2 Model set up

3.3.2.1 Physical model

The ideal wood block for the 2D heat transfer model is illustrated as following:

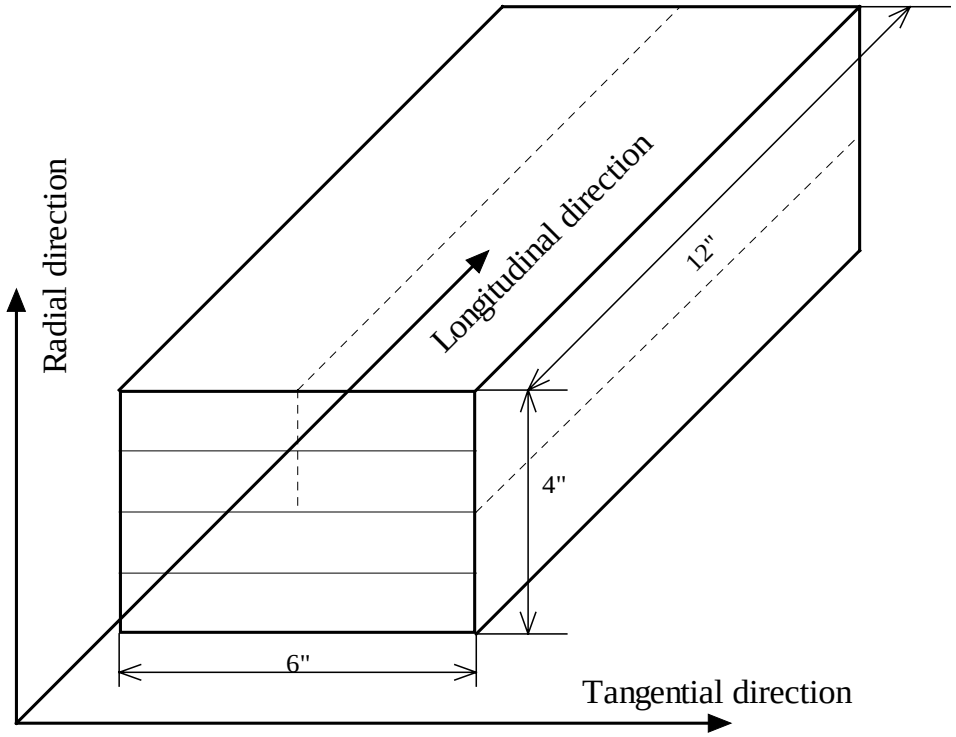

Figure 3. 2 The ideal wood block for modeling, and the direction notation and dimensions.

One 4"×6"×12" (102mm×152mm×305mm) wood block is modeled with the free convective boundary conditions on all sides of the block. The block was assumed to have the ideal ring orientation as shown in the Figure 3.2: On the cross section, the rings are oriented parallel to the top and bottom faces, which gave the perfect radial and tangential direction for the modeling. The two dimensional model is for the radial and tangential direction as shown. Since the boundary conditions on the four sides are assumed to be the same based on the symmetry

nature, only 1/4 of the block (as shown by the dotted line in the Figure 3.2) will be modeled for examining the transient temperature distribution in wood during the heat process.

3.3.2.2 Mathematical model

For modeling heat conduction in a material, the energy conservation law (the first law of thermodynamics) is applied. At a time instance t, the energy conservation law for a control volume (shown as in Figure 3.3) is expressed as:

$$\dot{E}_{st} = (\dot{E}_{in} - \dot{E}_{out}) + \dot{E}_{g}$$

Equa (3. 4)

where, $\dot{E}_{st}$ ---- Rate of energy stored at time t; = $\int_V \rho C_p \frac{\partial T}{\partial t} dV$;

ρ ---density;

C_p ---- specific heat;

V ---- volume of the control volume;

$(\dot{E}_{in} - \dot{E}_{out})$ ---- Net rate of energy crossing the surface of the control volume;

$\dot{E}_{g}$ ---- Rate of heat generation in the control volume;

Then apply the energy conservation to a differential control volume inside a solid (as shown in Figure 3.3):

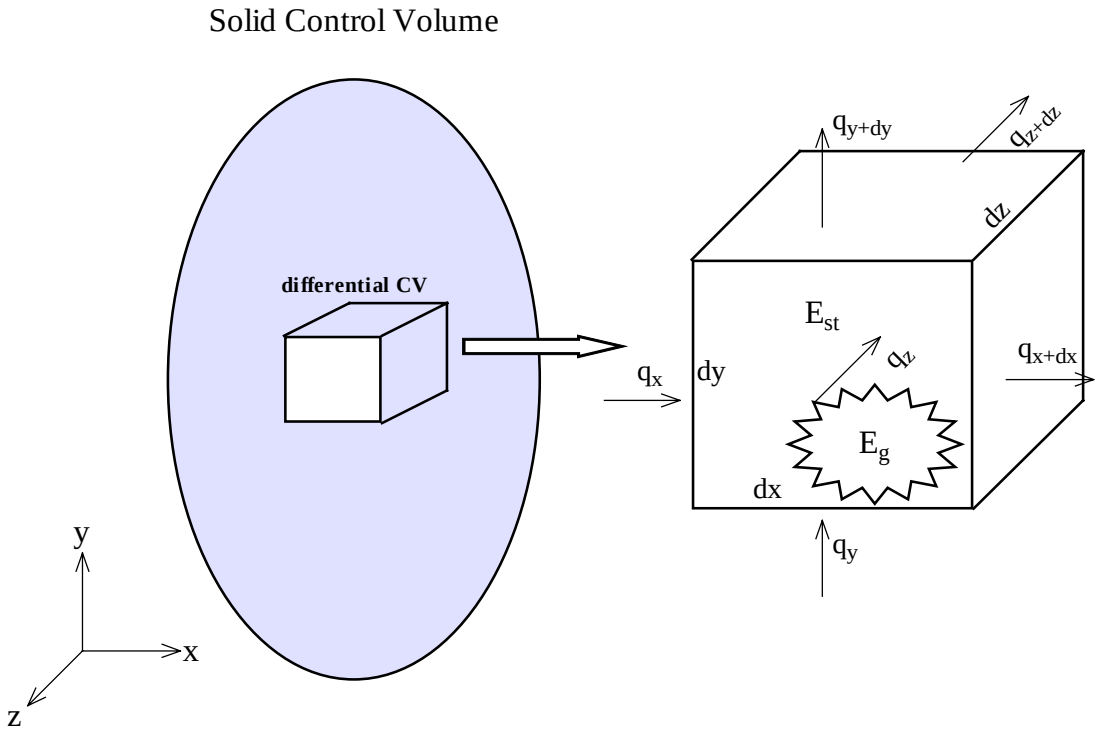

Figure 3. 3 Illustration for the energy conservation law on the control volume

$$\dot{E}_{in} - \dot{E}_{out} = q_x - q_{x+dx} + q_y - q_{y+dy} + q_z - q_{z+dz}$$
$$= q_x - (q_x + \frac{\partial q_x}{\partial x} dx) + q_y - (q_y + \frac{\partial q_y}{\partial y} dy) + q_z - (q_z + \frac{\partial q_z}{\partial z} dz)$$
$$= -\frac{\partial}{\partial x}[-k_x (dy \cdot dz)\frac{\partial T}{\partial x}] \cdot dx - \frac{\partial}{\partial y}[-k_y (dx \cdot dz)\frac{\partial T}{\partial y}] \cdot dy - \frac{\partial}{\partial z}[-k_z (dy \cdot dx)\frac{\partial T}{\partial z}] \cdot dz$$

Equa (3. 5)

(the last step was obtained by using Fourier's law)

$$\dot{E}_g = g \cdot dV$$

Equa (3. 6)

where, g = Energy generation rate per volume;

$$\dot{E}_{st} = \rho C_p \frac{\partial T}{\partial t} dxdydz$$

Equa (3. 7)

Substitute *Equa.(3.5), (3.6)* and *(3.7)* into *Equa. (3.4),* and divided by the differential volume, *dxdydz*:

$$\frac{\partial}{\partial x}(k_x \frac{\partial T}{\partial x}) + \frac{\partial}{\partial y}(k_y \frac{\partial T}{\partial y}) + \frac{\partial}{\partial z}(k_z \frac{\partial T}{\partial z}) + g = \rho C_p \frac{\partial T}{\partial t}$$

Equa (3. 8)

This is the partial differential equation for heat conduction in the three dimensions. Based on the assumptions for the two dimensional model, we can simplify to:

$$\frac{\partial}{\partial x}(k_x \frac{\partial T}{\partial x}) + \frac{\partial}{\partial y}(k_y \frac{\partial T}{\partial y}) = \rho C_p \frac{\partial T}{\partial t}$$

Equa (3. 9)

This is the mathematical model for our two dimensional heat transport in wood. The two directions x and y refer to the radial and tangential direction in wood shown in the Figure 3.2. The k_x and k_y are the thermal conductivity in the two respective directions. Values for these two parameters can be obtained from the geometric model predictions developed in the previous chapter. They are also functions of temperature as the experiments showed in the previous chapter. ρ is the density of block. Its value can be calculated from the specific gravity and moisture content according to the equation provided by the Wood Handbook (1999):

$$\rho = 1000 \cdot G_m \cdot (1 + M/100)$$

Equa (3. 10)

Where, G_m ---- specific gravity at certain moisture content;

M ---- moisture content;

Using the ovendry condition as it is modeled in the following, density can be calculated by simply multiply the ovendry specific gravity of the wood species by 1000. The heat capacity C_p for the ovendry wood species is a function of temperature based on several studies (Hearmon &Burcham 1955, McMillin 1969, Kock 1969, Kollmann 1962). But for simplification of the program in this study, C_p was specified as a constant value obtained from Incropera & DeWitt (1981) table 3:

C_p = 2805 kJ/kg.K @ T = 300K for the yellow pine cross grain.

3.3.2.3 Boundary and Initial conditions

3.3.2.3.1 Boundary conditions

As described in the physical model, there are two external boundaries at the top surface and edge and two internal boundaries at the symmetry planes. The two symmetry planes have zero heat flux as the boundary condition based on the symmetry character. The external boundaries are free convective heat flow with the convective heat transfer coefficient depending on the air flow above the external planes and the geometry of the external planes. Assuming the symmetry planes are at x=0 and y=0, and the two surfaces are at x=3" (76mm) and y=2" (50mm), the mathematical expression for the boundary conditions are:

$$
\begin{aligned}
q_x^{"} &= \frac{\partial T}{\partial x} = 0, && @\ x = 0mm;\\
k_x \frac{\partial T}{\partial x} &= h_\infty (T_\infty - T), && @\ x = 76mm;\\
q_y^{"} &= \frac{\partial T}{\partial y} = 0, && @\ y = 0mm;\\
k_y \frac{\partial T}{\partial y} &= h_\infty (T_\infty - T), && @\ y = 50mm;
\end{aligned}
$$

Equa (3. 11)

h_∞ can be calculated according to the method for external flow over a flat plate (Incropera & DeWitt 1981) with knowledge of the fluid properties, conditions and flow geometry. The flow medium is dry air. Properties of air for calculating the heat convection coefficient (h_∞)can be obtained from Table A.4 in Incropera & DeWitt (1981). For the air at a temperature of 100°C (373°K) and under 1 *atm* pressure, the required properties are:

ν = 23.665×10^{-6} (m^2/s);

k = 0.0319 (W/m.K);

Pr = 0.695;

Where, ν ---- kinematic viscosity of air;

k ---- thermal conductivity of air;

Pr ---- the Prandtl's number;

To determine the appropriate convection correlation (laminar flow or turbulent flow) for computing the average convection coefficient h, the Reynolds number must first be determined:

$$\mathrm{Re}_{top} = \frac{u_\infty \cdot W}{\upsilon} = \frac{0.5(m/s)\times 0.15(m)}{23.665\times 10^{-6}(m^2/s)} = 3169;$$
$$\mathrm{Re}_{side} = \frac{u_\infty \cdot H}{\upsilon} = \frac{0.5(m/s)\times 0.1(m)}{23.665\times 10^{-6}(m^2/s)} = 2113;$$

Equa (3. 12)

where, u_∞ ---- free flow velocity; 0.5m/s was obtained by measuring an ordinary drying oven while it was under the working condition;

W ---- width of the block;

H ---- height of the block;

The Reynolds numbers for flow on top and at the side are lower than the critical transition number ($5x10^5$). So both flows are laminar within the boundary layers, and the correlation for the laminar flow is used to calculate the Nusselt's number and the convection coefficients:

$$\overline{Nu_{top}} = 0.664\cdot \mathrm{Re}_{top}^{1/2}\cdot \mathrm{Pr}^{1/3} = 0.664\cdot (3169)^{1/2}(0.695)^{1/3} = 32.53;$$
$$\overline{Nu_{side}} = 0.664\cdot \mathrm{Re}_{side}^{1/2}\cdot \mathrm{Pr}^{1/3} = 0.664\cdot (2113)^{1/2}(0.695)^{1/3} = 26.56;$$

Equa (3. 13)

and the average convection coefficients are then calculated by:

$$\overline{h_{top}} = \frac{\overline{Nu_{top}} \cdot k}{W} = \frac{32.53 \times 0.0319 W/m \cdot K}{0.15m} = 6.92 (W/m^2 \cdot K);$$

$$\overline{h_{side}} = \frac{\overline{Nu_{side}} \cdot k}{H} = \frac{26.56 \times 0.0319 W/m \cdot K}{0.1m} = 8.47 (W/m^2 \cdot K);$$

Equa (3. 14)

3.3.2.3.2 *Initial condition*

Initially the temperature in the wood block was assumed to be room temperature, which is about 24°C.

$$T = T_i \qquad @t = 0;$$

Equa (3. 15)

Where, T_i ---- the initial temperature (°C).

3.3.3 Numerical analysis and solutions

When the problems are dealing with complicated geometry or nonlinear properties, exact analytical solutions usually become difficult as impossible. Numerical solution is an approximate solution for the problem at a finite number of points. It is easy and possible. When the analytical solution -- an exact solution over the entire domain -- for the model (Equa.3.9, 3.11 and 3.15) described above is not possible due to non-linearity, a numerical solution is sought for solving the model. Finite difference(FD), Finite element (FE) and Boundary element (BE) methods are popular techniques for numerically solving the heat and mass transfer problems. Each method has its own advantages and disadvantages. Finite Difference method is convenient for solving 2D or 3D problems with regular shapes, and it is conceptually simple . It involves discretizing the governing equations for the control volume. Finite Element method is more suitable for complicated geometric problems but conceptually difficult. It is based on the weak or variational

form of the equations. Boundary Element method is also for complicated geometry. Mathematically it is much more difficult than FD and FE method because it uses the free space Green's Functions to derive integral equations.

Finite difference method applied to a control volume is used here to solve the model. Discretization of the control volume is described next (from Vick's class hand-outs, 1999).

3.3.3.1 Discretization for the internal equation

The two-dimensional domain is discretized as shown in Figure 3.4. The whole domain is completely filled with control volumes (CVs) and grid points with zero thickness CVs are placed on the boundaries. The heat flow on the four sides of each inside CV, such as (m,n), is shown in Figure 3.5.

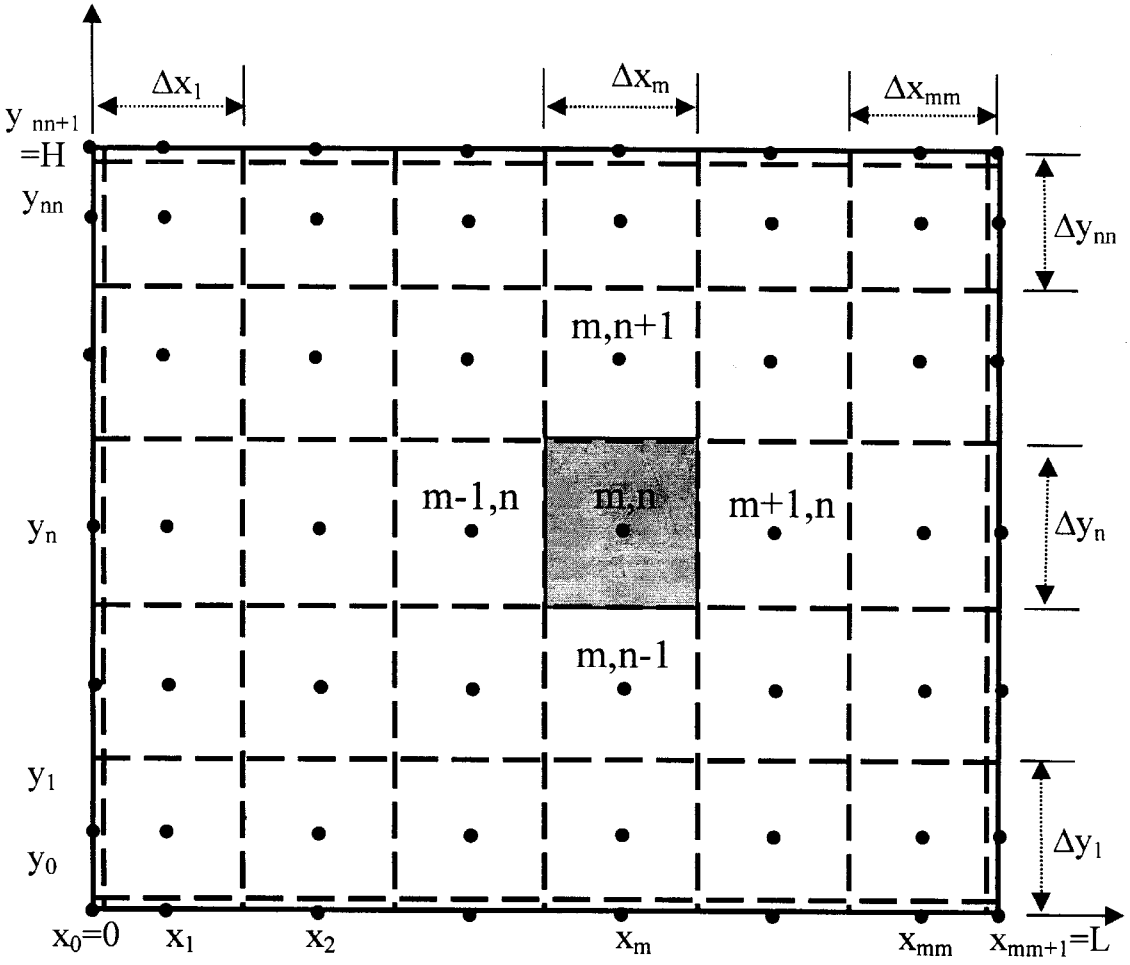

Figure 3. 4 Illustration for the control volume discretization. (Vick 1999).

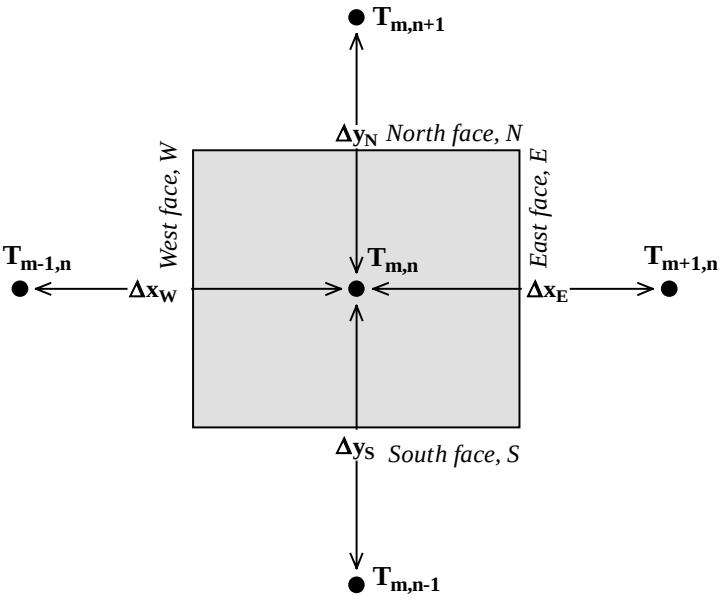

Figure 3. 5 Illustration of the heat flow for the small control volume.

Notation:

m	integer indicator in x-direction for a small CV;
mm	total number of CV's in the x-direction;
Δx_m	x-direction length of the small CV "m,n";
x_m	x-location of the center of the small CV "m,n";
n	integer indicator in y-direction for a small CV;
mm	total number of CV's in the y-direction;
Δy_n	y-direction length of the small CV "m,n";
y_n	y-location of the center of the small CV "m,n";
E	designated the east side face of the CV;
W	designated the west side face of the CV;
N	designated the north side face of the CV;
S	designated the south side face of the CV;
$T_{m,n}$	temperature at the center of CV "m,n";

$$\Delta x_E = \frac{\Delta x_m}{2} + \frac{\Delta x_{m+1}}{2}$$

= distance between the center of CV "m,n" and its east neighbor "m+1,n";

$$\Delta x_W = \frac{\Delta x_{m-1}}{2} + \frac{\Delta x_m}{2}$$

= distance between the center of CV "m,n" and its west neighbor "m-1,n";

$$\Delta y_N = \frac{\Delta y_n}{2} + \frac{\Delta y_{n+1}}{2}$$

= distance between the center of CV "m,n" and its north neighbor "m,n+1";

$$\Delta y_S = \frac{\Delta y_{n-1}}{2} + \frac{\Delta y_n}{2}$$

= distance between the center of CV "m,n" and its south neighbor "m,n-1";

The model equation (Equa.3.9) is integrated over the control volume (m,n):

$$\int_{t=t_{p-1}}^{t=t_p} \int_S^N \int_W^E [\frac{\partial}{\partial x}(k_x \frac{\partial T}{\partial x}) + \frac{\partial}{\partial y}(k_y \frac{\partial T}{\partial y}) - \rho C_p \frac{\partial T}{\partial t}] dx dy dt = 0;$$

Equa (3. 16)

After performing the integration, (the complete integration process is shown in the Appendix B) the discretized equation can be written in the form:

$$a_{m,n}T^p_{m,n} - aW_{m,n}T^p_{m-1,n} - aE_{m,n}T^p_{m+1,n} - aS_{m,n}T^p_{m,n-1} - aN_{m,n}T^p_{m,n+1} = b_{m,n}$$

Equa (3. 17)

Where,

$$aW_{m,n} = \frac{k_{Wx}}{\Delta x_W}\Delta y_n = \Delta y_n\left(\frac{k_x}{\Delta x_m + \Delta x_{m-1}/2}\right);$$

$$aE_{m,n} = \frac{k_E}{\Delta x_E}\Delta y_n = \Delta y_n\left(\frac{k_x}{\Delta x_m + \Delta x_{m+1}/2}\right);$$

$$aS_{m,n} = \frac{k_S}{\Delta y_S}\Delta x_m = \Delta x_m\left(\frac{k_y}{\Delta y_n + \Delta y_{n-1}/2}\right);$$

$$aN_{m,n} = \frac{k_N}{\Delta y_N}\Delta x_m = \Delta x_m\left(\frac{k_y}{\Delta y_n + \Delta y_{n+1}/2}\right);$$

$$aO_{m,n} = (\rho C_p)\frac{\Delta x_m \cdot \Delta y_N}{\Delta t_p};$$

$$a_{m,n} = aO_{m,n} + aW_{m,n} + aE_{m,n} + aS_{m,n} + aN_{m,n};$$

$$b_{m,n} = aO_{m,n} \cdot T_{m,n}^{p-1};$$

3.3.3.2 Discretization for the boundary condition

The boundary node shown on the 2-dimensional grid (Figure 3.4) is surrounded by an imaginary control volume with zero volume. All but one neighbor coefficient is zero on each boundary. For completeness of the program (written for the model in the following), boundary conditions were not limited to the conditions specified for the physical model (Figure 3.2) developed above, but rather a complete set with the combination of specified heat flux for the boundary (with the knowledge of q'') and specified convective boundary (with the knowledge of h_∞ and T_∞).

Boundary at x=0 (m=0)

The boundary condition for the combination of specified heat flux , *qx0*, and convective conditions, *T∞x0* and *hx0*, can be written in the form:

$$-k_x \frac{\partial T}{\partial x} = qx0 + hx0 \cdot (T\infty x0 - T), \quad at\ x = 0;$$

Equa (3. 18)

The discretized form of this boundary condition is, (k_x is constant with respect to the location)

$$k_x \frac{T_{0,n}^p - T_{1,n}^p}{\Delta x_1 / 2} = qx0 + hx0_n \cdot (T\infty x0_n - T_{0,n}^p);$$

Equa (3. 19)

The discretized equation can be expressed in terms of coefficients as:

$$a_{0,n} \cdot T_{0,n}^p - aE_{0,n} \cdot T_{1,n}^p = b_{0,n}$$

Equa (3. 20)

Note that $aW_{0,n}$ is not needed at this boundary since there is no west neighbor. These coefficients are:

$$aE_{0,n} = \frac{k_x}{\Delta x_1 / 2};$$
$$a_{0,n} = aE_{0,n} + hx0_n;$$
$$b_{0,n} = qx0 + hx0_n \cdot T\infty x0_n;$$

If the boundary condition is a specified surface temperature, $Tx0_n$, we have the special case with:

$aE_{0,n} = 0,\ a_{0,n} = 1,\ b_{0,n} = Tx0_n$

Now we have three types of boundary conditions. We use an indicator to keep a record of the type of boundary condition we have for later programming:

1. Specified temperature (Tx0 known);

BCx0 == 2. Specified heat flux (qx0 known, hx0=0, T∞x0=0);

3. Specified convection (hx0 and T∞x0 known, qx0=0);

For the model studied in this project, the boundary condition at x=0 is the second type boundary condition with specified heat flux *qx0*=0.

Boundary at x=L (m=mm+1)

A similar derivation is used for the coefficients at boundary x=L as for the coefficients at x=0, but with different subscripts and change $aE_{0,n}$ to $aW_{0,n}$, because there is no east neighbor at this boundary. The result form is:

$$a_{mm+1,n} \cdot T^{p}_{mm,n} - aW_{mm+1,n} \cdot T^{p}_{mm+1,n} = b_{mm+1,n};$$

Equa (3. 21)

$$aW_{mm+1,n} = \frac{k_y}{\Delta x_{mm} / 2};$$

Where, $a_{mm+1,n} = aW_{mm+1,n} + hxL_n;$

$$b_{mm+1,n} = qxL_n + hxL_n * T\infty xL_n;$$

The same boundary indicator was used to distinguish three different boundary conditions:

BCxL=1,2,3 corresponding to the specified temperature boundary, the specified heat flux, and the specified convective boundary. For the model in this study, the boundary condition at x=L is the third type boundary with the specified convective boundary.

Boundary at y=0 (n=0)

Similar as x=0:

$$a_{m,0} \cdot T^{p}_{m,0} - aS_{m,0} \cdot T^{p}_{m,1} = b_{m,0};$$

Equa (3. 22)

$$aS_{m,0} = \frac{k_y}{\Delta y_1 / 2};$$

Where, $a_{m,0} = aS_{m,0} + hy0_m;$

$$b_{m,0} = qy0_m + hy0_m * T\infty y0_m;$$

Boundary at y=H (n=nn+1)

Similar as x=L:

$$a_{m,nn+1} \cdot T^p_{m,nn} - aN_{m,nn+1} \cdot T^p_{m,nn+1} = b_{m,nn+1};$$

Equa (3. 23)

$$aN_{m,nn+1} = \frac{k_y}{\Delta y_{nn} / 2};$$

Where, $a_{m,nn+1} = aN_{m,nn+1} + hyL_m;$

$$b_{m,nn+1} = qyL_m + hyL_m * T\infty yL_m;$$

3.3.3.3 Time discretization

A fully implicit scheme was used for the time discretization during the above integration process for the space discretization (see details in Appendix B). The fully implicit scheme is much superior to the explicit and center difference schemes, which were commonly used. The explicit scheme has stability problems if the time step is too large. The center difference scheme is reported to be "unconditionally stable" in most books. But according to Vick (1999), the statement is wrong, and the center difference scheme in fact suffers from damped but still nonphysical oscillations if the time step is too large. The time discretizatioin was also shown in the Appendix B for the model solved here.

3.3.3.4 Numerical solution

The number of equations which will be solved simultaneously depends on the grids on the control volume. The more tight the grid is, the more accurate the numerical solution is, but the more time the program will run in the computer. The number of simultaneous equations is typically large, so the direct matrix inversion is not practical. Instead, iterative methods are usually employed.

A Line-by-line numerical method was used for solving this model. This method is a combination of the direct tridiagonal algorithm and Gauss-Siedel methods. The general idea for this Line-by-line method is illustrated in Figure 3.6. First choose a direction (for instance, y-direction) and assume neighbors at other x-locations are known from the previous iteration; then solve this line of nodes using the tridiagonal algorithm; then move or sweep to the other x-locations; and alternate the sweeps in the x and then the y-directions to accelerate convergence.

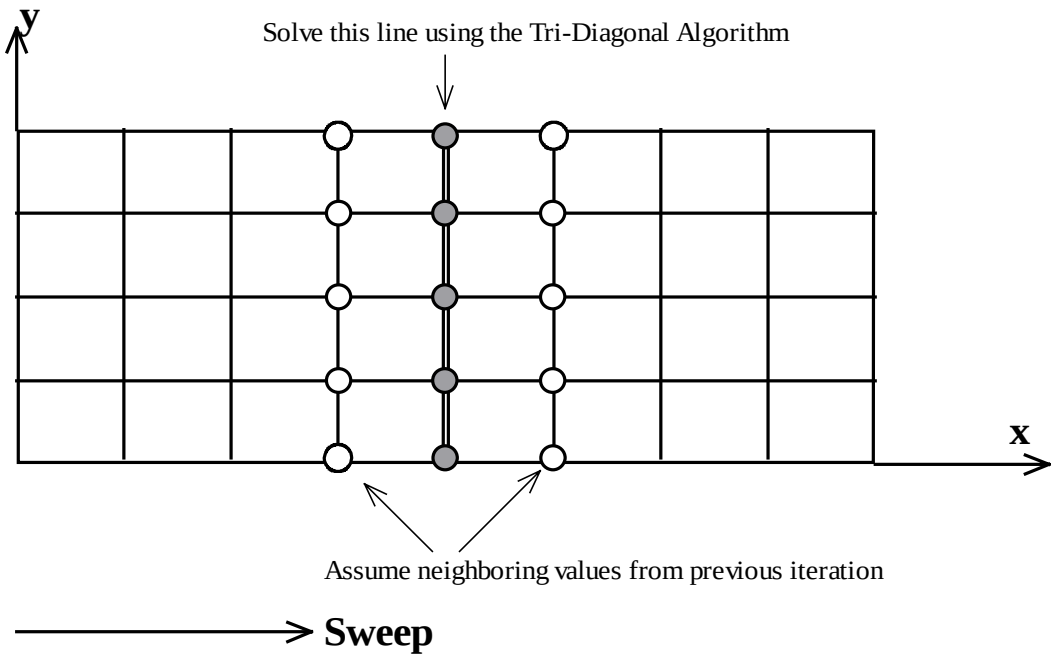

Figure 3. 6 illustration for the Line-by-Line numerical method used for solving the model.

The program was written in *Mathematica* software. A lot of built-in solvers, such as Tri-Diagonal solver, gave efficiency for programming. *Mathematica* adopts FORTRAN for the

programming which is simple and fast. Many options are provided for plotting the results. Powerful visualization for the results is the first reason for engineers to choose *Mathematica* as the scientific tool. Also with *Mathematica*, reports and partition of the program became clear and easy.

The program code is attached in Appendix B. There are four general sections in the program -- Add-in section for calling some packages built-in *Mathematica* and specifying plot options; User input section (for making any required changes on the input by users), Computations (the heart of the program), and Results (for data output and plots). Clear lay-out is easy for people with different interests to get into the specific part of the program.

The user input section is designed for easy modification by users. The program is designed for a general 2-dimensional model with different kinds of boundary conditions. The boundary conditions in the program were written for easy selection by users from one of the three types of boundary conditions described in the previous section. Geometry of the sample and the number of mesh are easy and clear for users to modify. Time discretization can also be modified by users. Some constant property values are required for the material to be modeled.

The computation section is easy for the programmers to modify. Some documentationis provided for each subsection code.

Results are the most interested part. Temperature distribution in the two directions with the change of time can be shown and animated. Temperature profiles in the two directions can be compared in one plot with animation. Transient temperature profile (temperature plotted as a function of time) at a certain location can be shown easily.

The 2D transient anisotropic heat conduction model for a sample of wood was solved by the program developed in the *Mathematica* in 5 minutes with the mesh of 11×11 on the cross section of a wood block. Results of a model simulation run are shown and discussed in the following section.

3.3.4 Results and Discussions

The described program can predict the transient temperature profiles in any two specified directions with different heat transfer coefficients. In the pure heat conduction model, the heat transfer coefficient is the thermal conductivity. Different thermal conductivity in the two directions gave different temperature profiles in the two directions. The temperature dependent thermal conductivity made the temperature profile change non-linearly with time.

In this study, the model is used to predict the temperature profile in the radial and tangential directions since the heat transfer mainly occurs in these two directions when wood is subjected to a heating process. Thermal conductivity values in the two specified directions -- radial and tangential --were derived in the last chapter by the anatomical structure observation and geometrical models. Relations between thermal conductivity in each direction with the average temperature were obtained from the last chapter, too, by regression analysis of the testing results. They were used in the program for solving the model.

3.3.4.1 Simulation run

Mathematical modeling and numerical simulation can provide crucial information about the physical mechanisms for the phenomenon, such as drying wood (Turner 1996). The fundamental knowledge gained from analyzing the numerical results allows better understanding of heat or mass transfer phenomenon.

A model simulation was run on a southern yellow pine wood block. Geometry of the block is defined as the dimension shown in the Figure 3.2. However, since the simulation is to examine the different thermal conductivities' affect on the heat transportation in the two directions, the same dimension for the two directions (radial and tangential) on the block was assumed in the simulation run in order to make the comparison based on the same distance for the heat transfer in the two directions. Simulation is for the ovendry wood sample. Density of southern yellow pine at the ovendry condition was found to average 600 kg/m^3 (Haygreen & Bowyer 1982). It has been shown that wood specific heat is a function of temperature (Skaar 1988). But a constant average value of 2805 (kJ/kg·K) is used in the program for the simulation as obtained from Incropera & DeWitt (1981). Later in the analysis of the results, it was found that the dependence for the specific heat on the temperature is very crucial to the model output. Therefore in the future, this 2D model should be modified for including the function of temperature for the specific heat.

The radial and tangential thermal conductivity were shown to be functions of temperature from the testing results in the previous chapter. Expressions were modified for Fahrenheit temperature and based on the initial value of k_t *and* k_r at temperature of 75°F (24°C):

$$k_t = 0.00028 * (T - 75) + 0.0837;$$
$$k_r = 0.00028 * (T - 75) + 0.1418;$$

Equa (3. 24)

The linear coefficient for the temperature in *Equa.3.24* was transferred from the coefficient obtained in the linear regression for the Centigrade temperature. The constant terms in the equations were obtained from the tables (table A-34, and A-35 in the Appendix A) predicted by the thermal conductivity geometrical models in the last chapter, and based on the 0% MC and 40% latewood.

The boundary and initial conditions were set up as the model described in section 3.3.2.3.

3.3.4.2 Heat transfer mechanism analysis

Simulations for heat transfer in the radial and tangential directions were displayed by a series of three-dimensional plots and contours plots from *Mathematica*. Transient temperature distribution changes were clearly observed from good graphical presentations. *Mathematica* software not only provides lots of graphic options but also animations, which is a great help for observing the dynamic process. Plots (Figure 3. 7 and 3.8) for the results from the simulation are more for qualitative than quantitative observations due to idealization of model geometry and utilization of theoretical values for the parameters in the model.

At the commencement of the heating process (time=0 sec), the temperature was uniformly distributed with the specified initial temperature (24°C or 75°F). Within a very short time, the temperature on the surface and at the edge increases sharply to equilibrate with the external environment temperature due to the high convective coefficients. From the graphs, it was obviously shown that heat flow transported from the outside to the inside with the whole temperature profiles increased with time until reaching equilibrium with the environment temperature (time= 20000 sec). The temperature increase fast at the beginning of the heating process with a steep temperature gradient in both directions (time=400 sec), and then slowed down due to the small temperature difference within the sample. It can be seen (but not as clear as the one-dimensional plots in the next section) that the temperature increased faster in the radial

direction than in the tangential direction due to the higher thermal conductivity value for the radial direction (Contour plots in Figure 3.7 and Figure 3.8). But the difference is not very significant since the ratio of the radial over tangential thermal conductivity values (theoretical) used in the simulation is only 2:1. This faster radial heat transfer was obviously shown at the early heating period (time=400 sec in Figure 3.7). In the end the temperature within the block became uniformly distributed as shown in the Figure 3.8 (time=20000 sec).

All the graphs were plotted in *Mathematica*, which has the best visualization effect for the model output. Not only can the graphs be displayed individually at each time step for detailed examination, but also they can be displayed together as an animation for the overall trend observation, which will be very helpful for the industry operators to easily foresee the overall changes of the process. *Mathematica* software also makes the online display and publication very convenient. The model in this study solved and plotted in the *Mathematica* will be easy and ready to be put on-line.

The 3D plots and contours plots for temperature profiles are powerful graphical tools that provide a better understanding of the relative change and changing patterns. However, it is difficult to analyze the details of the change and compare the heat transfer in the two directions.

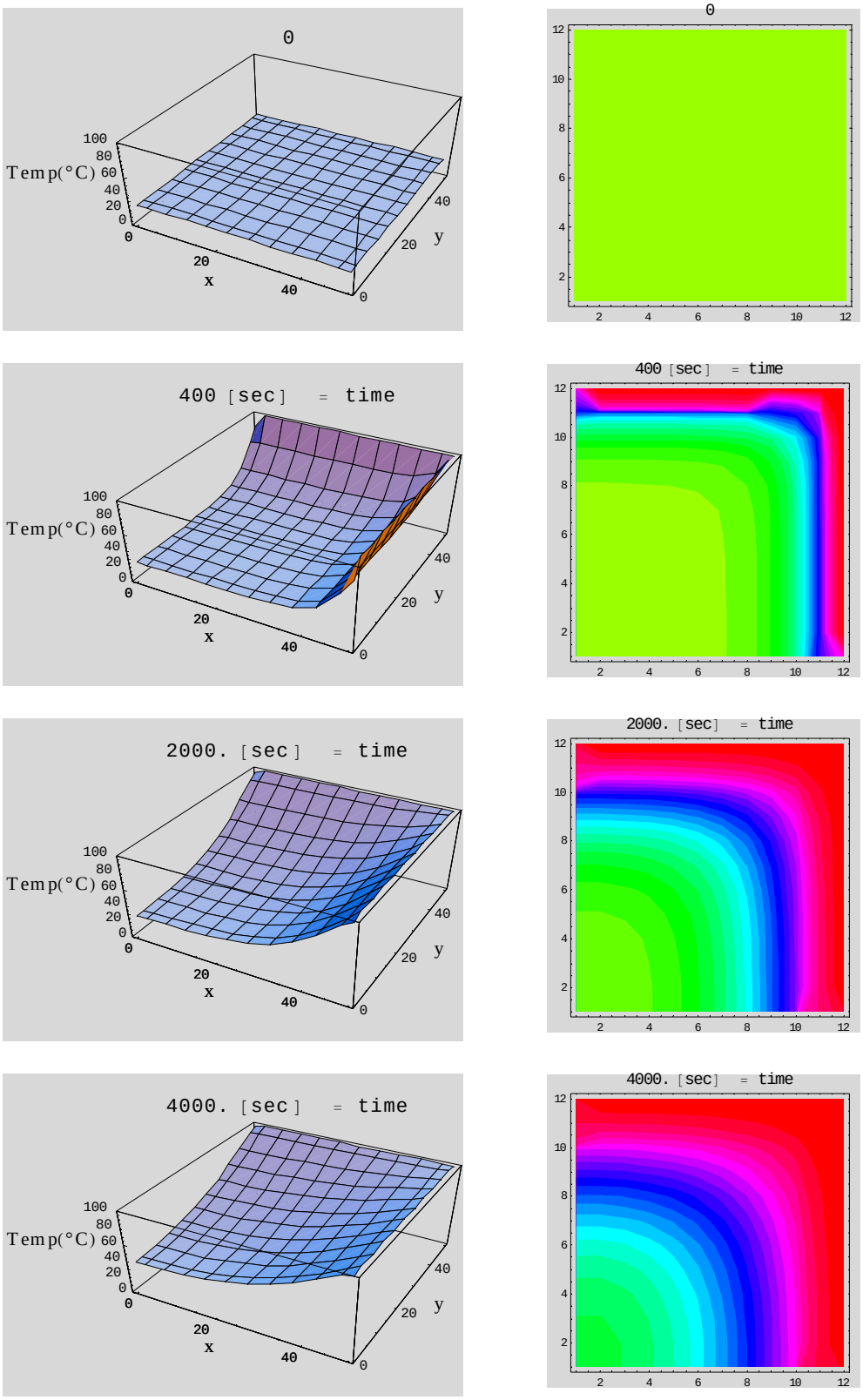

Figure 3. 7 3D plots and contour plots for the temperature distribution in change the two direction with time.

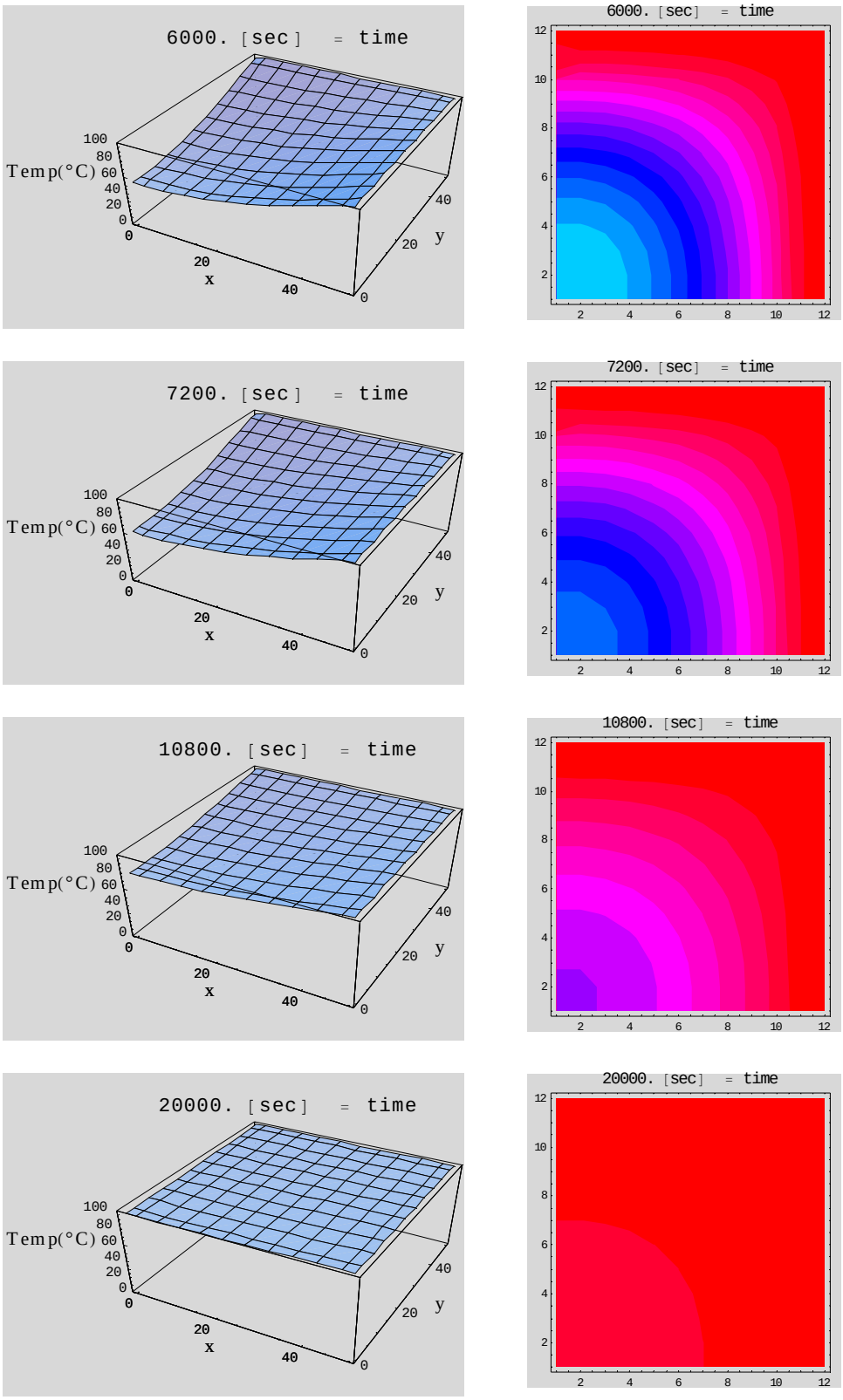

Figure 3. 8 3D plots and contour plots for the temperature distribution in change the two direction with time (continued).

3.3.4.2.1 *Time series analysis*

The 2D heat transfer simulation provides the temperature values at any point and any time. The information can be presented in many different ways. That temperature change at certain points with time is usually of interest to scientists and industry operators. Therefore the transient temperature profiles at specified points were plotted for the analysis. Before discussing the profiles, some notification for the point locations on the plane have to be clarified for simple reference in the following discussion. Figure 3.9 shows the definition for the points and plane locations.

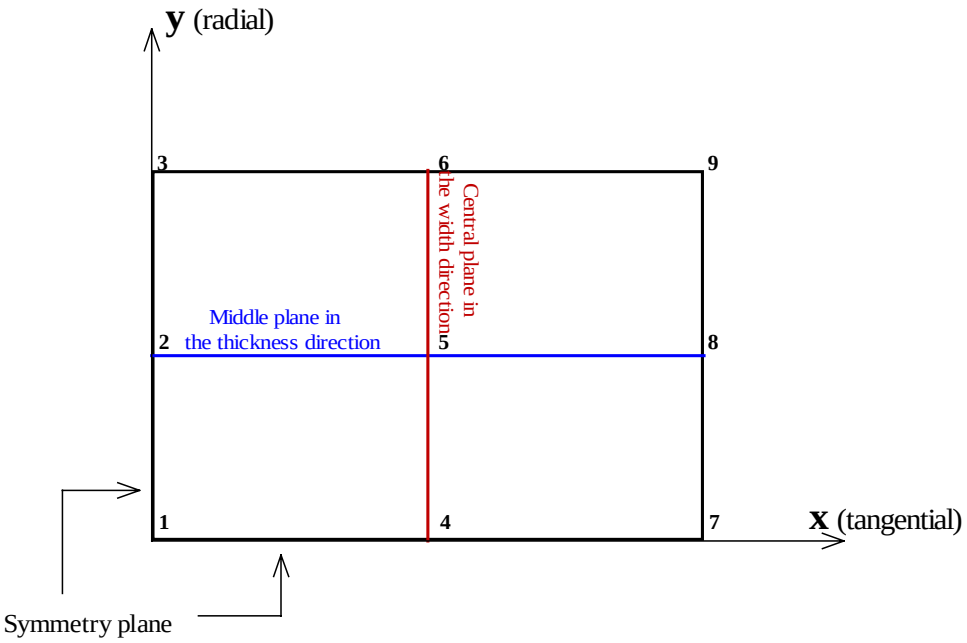

Figure 3. 9 Display of the points specified on the modeled transverse section of the wood block and the planes specified for the analysis.

Transient temperature profiles at points 1, 5 and 9 are shown in Figure 3.10. Temperature at the very outside point 9 increased dramatically to the environmental temperature once the heating process started. Temperature for the very inside point 1 did not change for the first 1000 seconds, then increased slowly with time until about 2500 seconds. After this time point, the temperature increase with time became relatively fast until it approached the boundary condition, then it slowed down again. Temperature at point 5 changed in the same style as the temperature at point 1, but with a faster increase for the whole time domain. After about 32,000 seconds (less than 10 hours), the temperature distribution within the block became uniform.

Three point temperature change profiles on the radial symmetry plane were plotted together with the other two points (points 4 and 7) on the tangential symmetry plane in Figure 3.11 to examine the different transfer rates in the two directions. It was shown that the temperature at point 2 (on the radial symmetry plane shown in Figure 3.9) is higher than the temperature at point 4 (on the tangential symmetry plane) after about 3 hours from the start of heating. Then the point 4 temperature increased quickly during the time between 2 to 5 hours since the heating started. It was even increased to a little higher than the temperature at point 2 until they both reached the boundary temperature. Same for the point 3 and point 7 temperature change but with very little difference between the temperature of these two points. They reached the boundary temperature within about 3 hours. Then they stayed at the boundary temperature for the rest of the heating process. Comparing temperature profiles of the three points on the radial symmetry plane with the profiles of the three points on the tangential symmetry plane, it can be seen that the temperature increases a little faster in the radial direction than in the tangential direction during the early heating process. Then in the later period, the tangential direction heat transport increased to keep up with the radial heat transportation until the whole temperature profile in the wood approached the boundary temperature, and the equilibrium state was reached.

Three different assumed convective coefficients (h_∞) at the boundaries were run in the simulation for examining the boundary condition effect on the heat transfer inside wood. First run was for the previously calculated convective coefficient ($h_{\infty,top}$ = 6.92W/m^2.K and $h_{\infty,side}$ = 8.47 W/m^2.K) as for the ordinary condition in the drying chamber. Second run was for an assumed *h* value of 100W/m^2.K, and the third run was for the assumed *h* value of 0.01W/m^2.K. The same five points (point 1,2,3 on the radial symmetry plane and point 4,5 on the tangential symmetry plane) temperature profiles were plotted for the three boundary conditions in Figure 3.12. The top two graphs were for the *h* value in the order of 10^1 and 10^2 magnitude. There was no big difference between these two graphs. The temperature profiles at all five points are almost equal for both model output runs by the program with the two different boundary convective coefficients. However, for the result from the model run with the *h* value in the order of 10^{-2} magnitude, temperature profiles are significantly lower than the other two conditions for all the five point temperatures. The temperature inside the wood block increased slower than the other two boundary conditions. And the temperature at the external point on the tangential symmetry plane (point 7) is higher than the temperature at point 3, the external point on the radial symmetry plane. This is contrary to the model results run for the *h* value in the order of 10^1 and 10^2. Temperature at point 4 (the middle point on the tangential symmetry plane) was lower than that at

point 2 (middle point on the radial symmetry plane) for the beginning (before time = 5,000 sec), then it increased over to the temperature at point 2. Therefore, it seems that heat transfers faster in the tangential direction than in the radial direction when the heat convection coefficient is very low at the boundary even though the tangential thermal conductivity is lower than the radial thermal conductivity. Observing the three graphs in Figure 3.12, it seems heat started transferring faster in the radial direction and followed with the tangential heat transfer catching up with the radial heat transfer. Then there was very little discrepancy between the radial and tangential temperature at the corresponding points, with tangential temperature profiles reaching the boundary temperature earlier than the radial ones.

From the analysis, we can see that changing the convective coefficients *h* at the boundaries has no effect on the internal heat transfer when the value is greater than 1. The calculated *h* value in this study was based on the air velocity of 0.5m/s at the boundaries. The *h* value is proportional to the free fluid velocity. Therefore any increase of the air flow velocity at the boundary has little effect on the internal heat transfer after it is over a specified limit, which means 0.5m/s air flow and 50m/s air flow at the boundary give the same results on the internal heat transfer. However, the increase of the air flow in the external environment may increase the internal moisture transportation rate, which will indirectly affect the heat transfer process in wood.

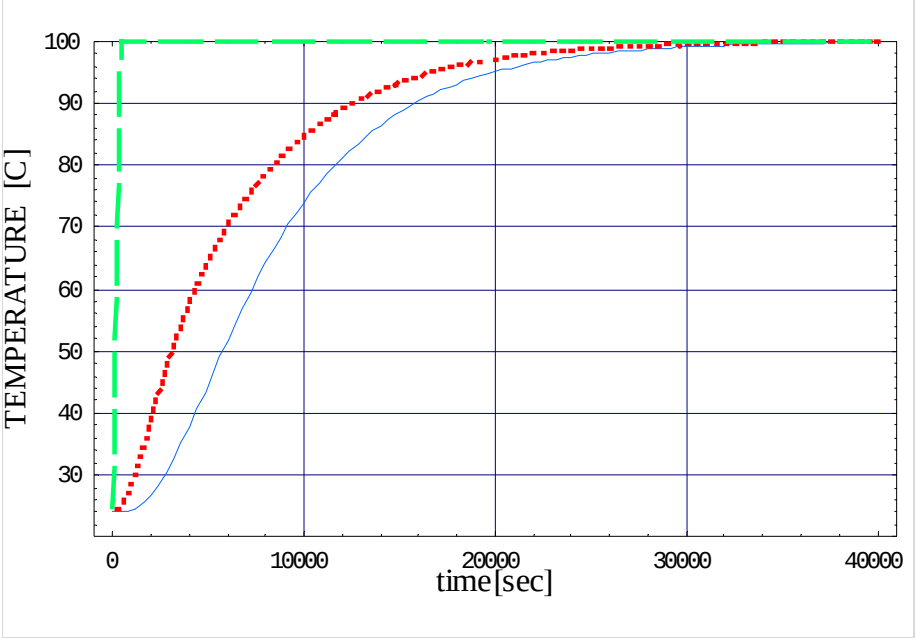

Figure 3. 10 Transient temperature profiles at point 1 (blue line), point 5 (red dotted line) and point 9 (green dashed line) predicted by the model simulation on southern yellow pine.

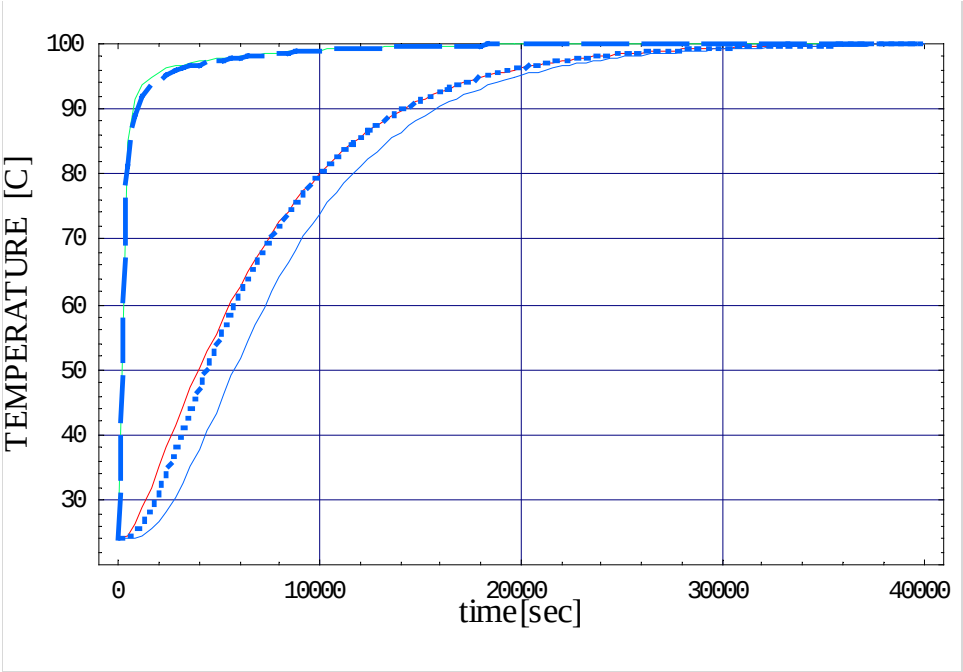

Figure 3. 11 Transient temperature profiles for the point 1 (blue line), 4 (blue dotted line) and 7 (blue dashed line) on the tangential symmetry plane, and for the point 2 (red line), point 3 (green line) on the radial symmetry plane.

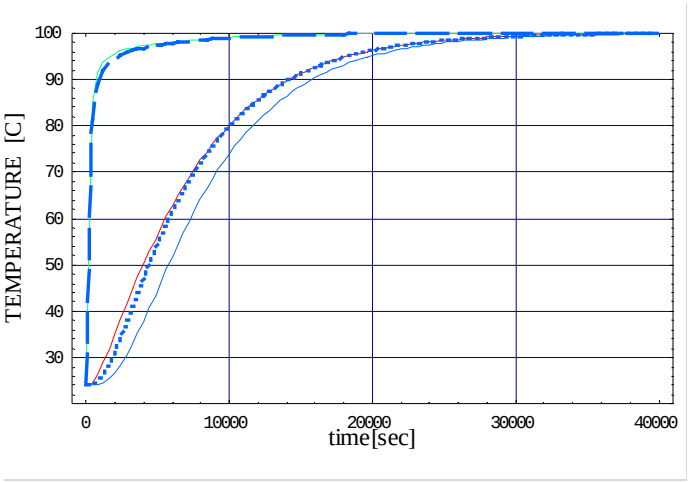

(a).

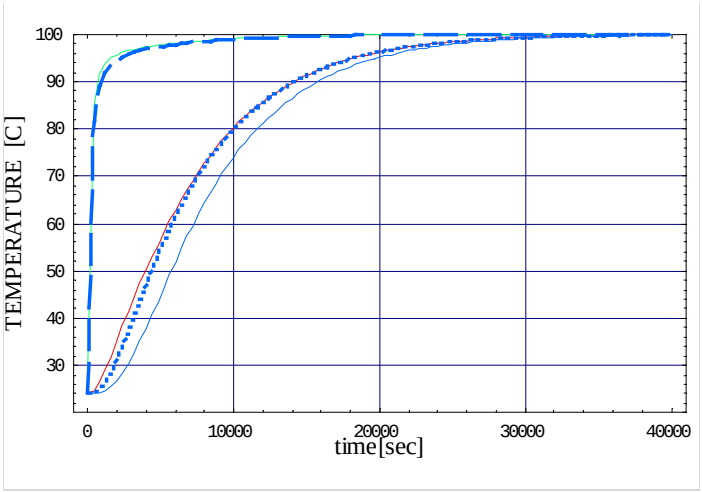

(b).

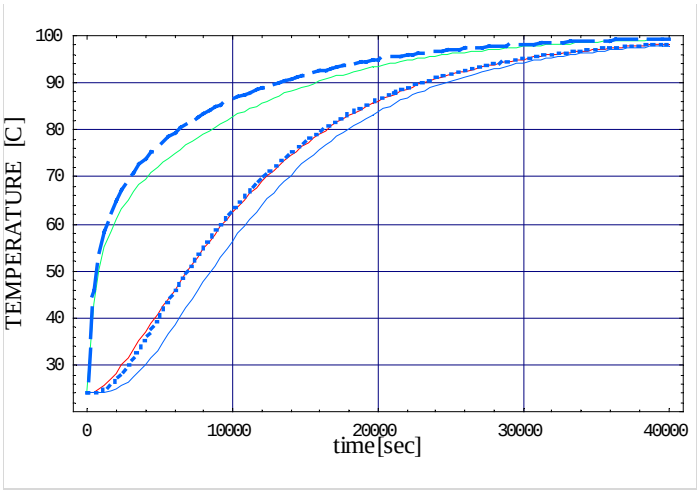

(c).

Figure 3. 12 The temperature profiles at the five points on the transverse plane predicted by the model with three different order of magnitude for the convective heat transfer coefficients at the boundaries: (a). $h_\infty \sim 10^1$; (b). $h_\infty \sim 10^2$; (c). $h_\infty \sim 10^{-2}$.

3.3.4.2.2 Spatial analysis

The temperature distribution change on the radial symmetry plane and on the tangential symmetry plane were shown in Figure 3. 13 and 3.14 at different specific times. And the temperature distribution change on the central plane in radial (vertical) direction (as illustrated in Figure 3.9 along 2, 5, 8 points) and on the middle plane in the tangential (horizontal) direction (along 4,5,6 points in Figure 3.9) were shown in Figure 3.15 and 3.16.

All the temperatures started at the initial temperature of 24°C. When the heat was applied to the wood block, temperature at the external points on the radial symmetry plane (point 3) and tangential symmetry plane (point 7) were increased by the affect of the boundary conditions. The very internal temperature at point 1 was not affected by the heating until a certain amount of time elapsed (~2,500 seconds). At the beginning of the heating process, the temperature differential in both directions was greater with steep slopes for the two temperature profiles, especially within the outside area near the boundary. With the time elapsed, the temperature differential in the two directions became less and less until all the temperatures inside the wood reached equilibrium with the boundary condition.

Comparing the temperature distribution in the two directions from Figure 3.13 and 3.14, it was shown that the radial temperature profile has a little steeper slope than the tangential temperature profile, but not significantly different. This is due to the higher thermal conductivity used for the radial direction heat transfer in the model than for the tangential direction.

The temperature distribution on the central plane in the radial (vertical) direction and on the middle plane in the tangential (horizontal) direction (Figure 3.15 and 3.16) show the same changing pattern as the two temperature distributions on the two symmetry planes discussed above. Temperature at the two external points for the radial and tangential plane equilibrates with the boundary temperature (100°C) immediately after the heating started. The inside point (between point 2 and 5 in Figure 3.9) temperatures (from x=0 to x< 25 mm) on the middle plane in the tangential direction were higher than the temperature within the corresponding range (between point 4 and 5) on the central plane in the radial direction. This was caused by the higher heat transfer rate (higher radial thermal conductivity) in the radial direction. Heat reaches the points between 2 and 5 faster by the radial flow than it reaches the points between 4 and 5 by the tangential flow. With the time passing, the internal area temperature on the central plane in the radial direction was increased to reach the same temperature of the corresponding area on the

middle plane in the tangential direction. And then the temperature in both directions approaches the boundary temperature with the same rate.

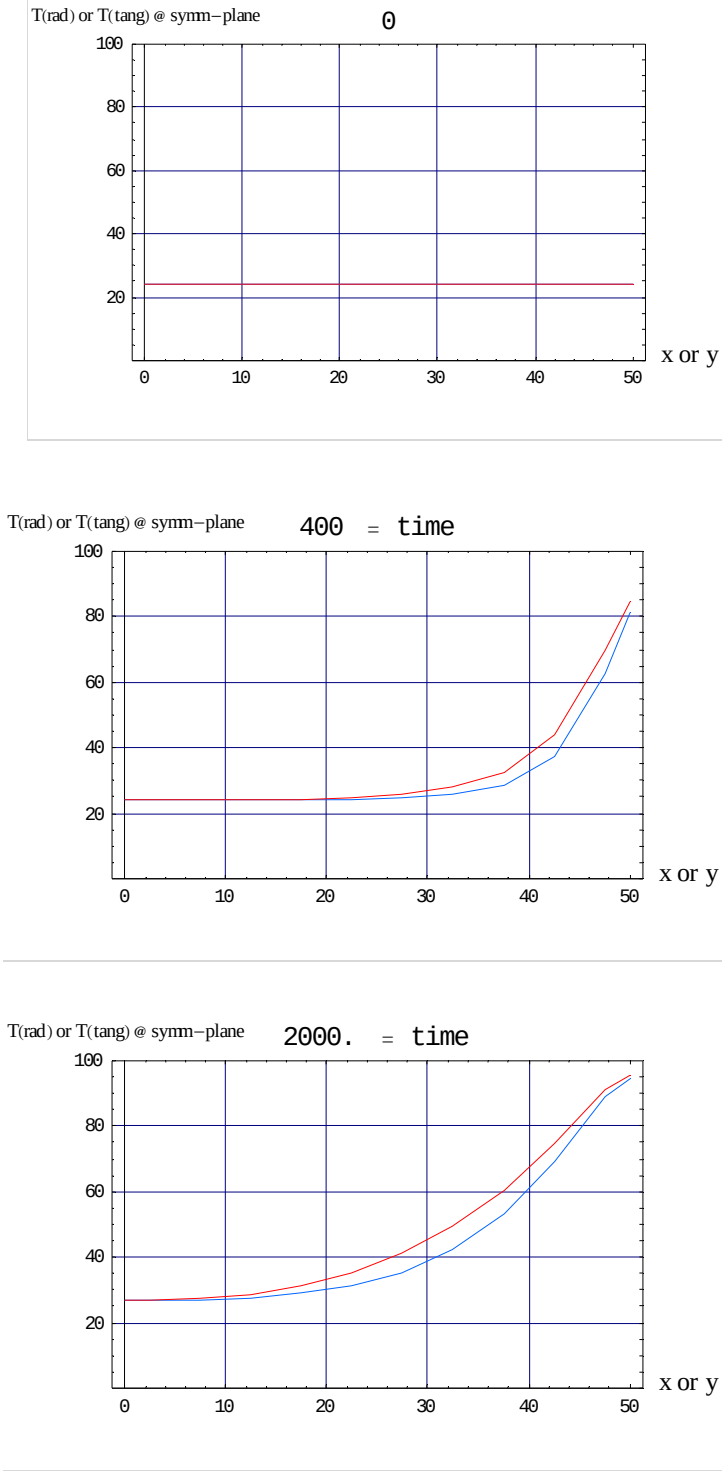

Figure 3. 13 Temperature distribution in the radial and tangential direction changes with time. Red line represents temperature profile on the radial symmetry plane; blue line represents the temperature profile on the tangential symmetry plane.

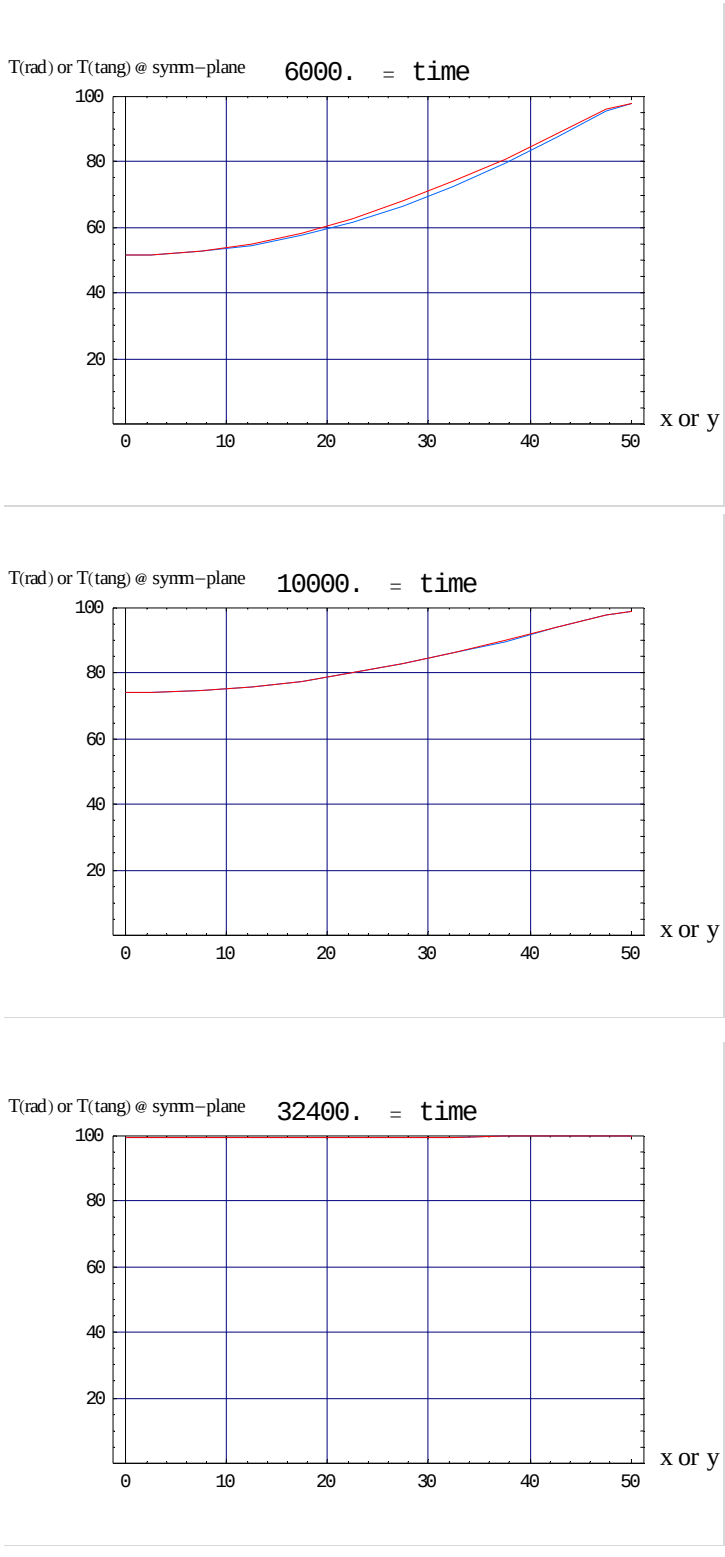

Figure 3. 14 (Continued) Temperature distribution in the radial and tangential direction changes with time. Red line represents temperature profile on the radial symmetry plane; blue line represents the temperature profile on the tangential symmetry plane.

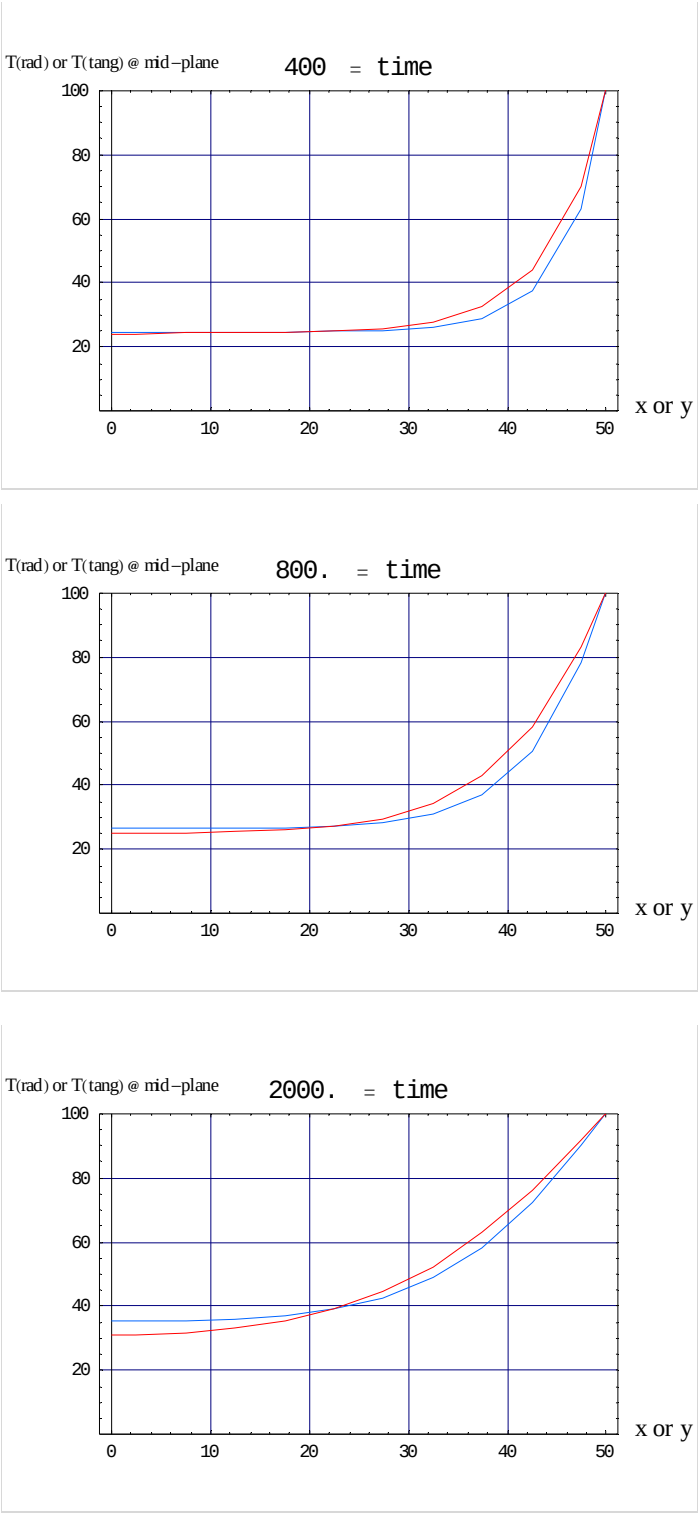

Figure 3. 15 Temperature distribution in the radial and tangential direction changes with time. Red line represents the radial temperature profile on the central plane (illustrated in Figure 3.9); blue line represents the tangential temperature profile on the middle plane (illustrated in Figure 3.9).

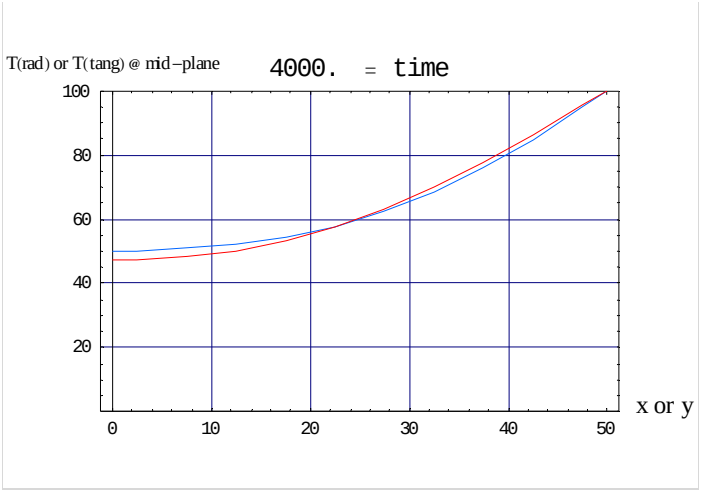

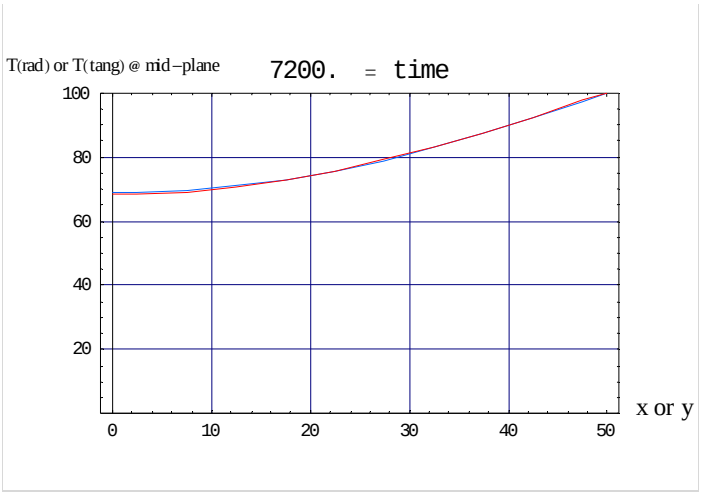

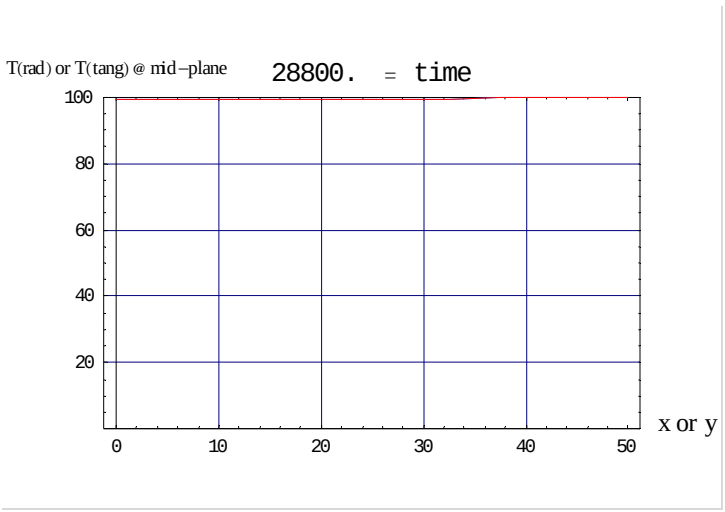

Figure 3. 16 (Continued) Temperature distribution in the radial and tangential direction changes with time. Red line represents the radial temperature profile on the central plane (illustrated in Figure 3.9); blue line represents the tangential temperature profile on the middle plane (illustrated in Figure 3.9).

3.4 Model evaluation and validation

The previous chapter described the anatomical structure affect, and the moisture and temperature affect on the two transverse thermal conductivities of wood. Theoretical derivation for the radial and tangential thermal conductivities gave the complete range of the values for the three species. The previous section (section 3.3) in this chapter provided a general 2D heat conduction model for the heat transport in any two directions with knowledge of the thermal conductivities in the specified directions. Here are some experimental tests for examining the model's (thermal conductivity geometrical model and 2D heat conduction model) capability to describe the heat transfer in different wood species with different structure and moisture content (MC).

3.4.1 Material and Methods

3.4.1.1 Sample preparation

Three species, southern yellow pine (*Pinus spp.*), Scots pine (*P.Sylvestra*) and soft maple (*Acer rubrum*), were chosen for the validation tests following the focus in this study. A southern yellow pine wood block was cut from a commercial 4x6 construction board. The true dimension of the block was 3.5"×5.5"×12" (90mm×140mm×305mm). The commercial board is usually dried to 12%MC. Scots pine samples were bought from Switzerland, with the true dimension of 4"×6"×12" (101mm×152mm×305mm). Samples with MC of 12% were wrapped in plastic to prevent any checks during the shipment. Moisture content of the samples was reexamined when they arrived here, and was between 10% to 14%, so there was no significant moisture desorption or absorption in the shipping. A sample block of the soft maple was cut from a green log bought from a local lumber yard. The moisture content of the sample was measured with the standard ovendry method described in any wood technology book. Testing samples were cut from the heartwood area of the log. Therefore the moisture content was measured as 35%. The dimension for the maple testing blocks is 4"×6"×12" (101mm×152mm×305mm).

Each block was put into a convection oven with temperature set at 100°C (or 60°C) for the heating process. Thermocouples were used for measuring the temperature at certain positions during the heating process. Nine 3/32"-diameter holes were drilled on each sample block at the approximate position specified in Figure 3.9, and the thermocouples were inserted into the holes for monitoring the temperature change at those positions.

Thermocouples were bought from the Omega Engineering Company. Hypodermic needle probes of type J thermocouples (shown in Figure 3.17) were chosen for the tests. A data acquisition system was built at Virginia Tech for automatic recording of temperatures from the thermocouples. Accuracy for type J thermocouples is ±1.1°C or ±0.4%. Accuracy for the data acquisition system was calculated based on specification of the acquisition board bought from the ComputerBoard Company. Absolute accuracy of the system is ±3.1°C for the worst case, and relative accuracy is ±0.4°C. Resolution for the acquisition system is ±0.1°C.

Figure 3. 17 Hypodermic thermocouples used in the test with 1/16" diameter of the probe. The temperature was measured only at the tip of the probes.

3.4.1.2 Experimental procedure

Each testing block with the nine thermocouples was put into the oven located at the Brooks Center, Virginia Tech (shown in the Figure 3.18). The oven was set at 100°C for heating the southern yellow pine and Scots pine wood blocks. The oven was set at 60°C for the maple sample to accommodate another test being run concurrently. Later in modeling for maple, the boundary condition was also set to be 60°C. A air flow inside the oven was measured for about 0.5m/s. Data for the temperature change at the nine points were continuously recorded for 3 hours to compare with the model predicted values.

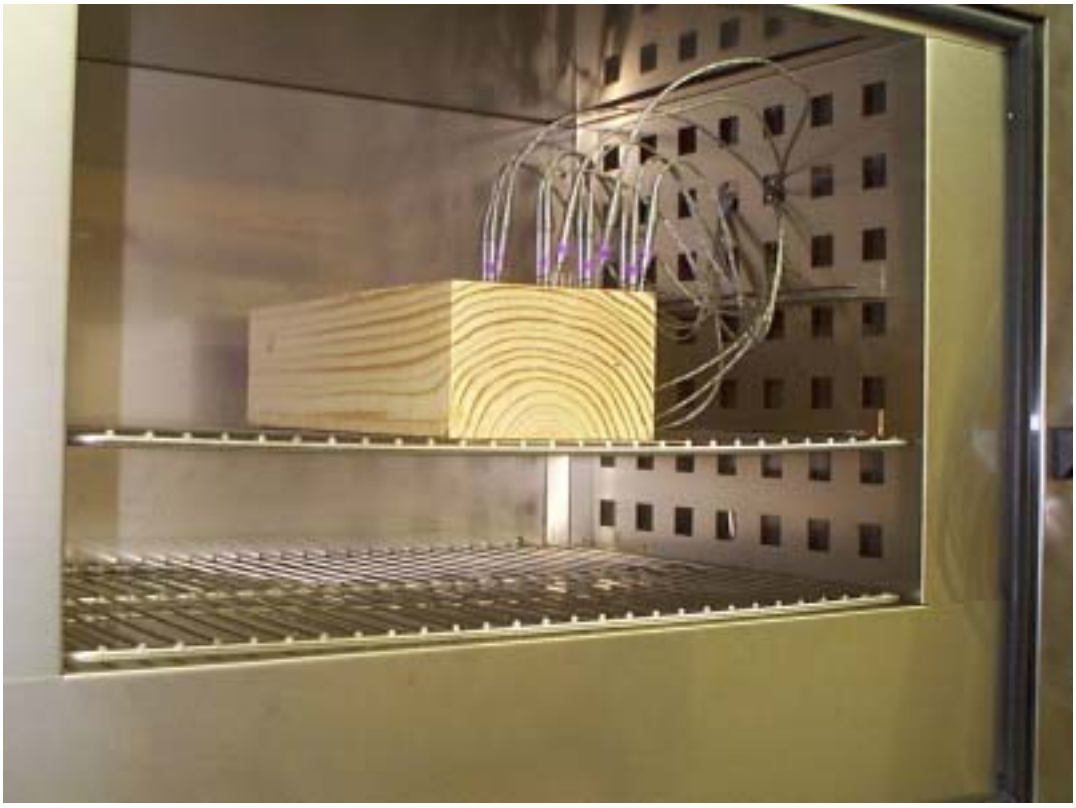

Figure 3. 18 Testing sample with the thermocouples was ready to be tested in the ordinary oven.

Each of the three species wood blocks was tested individually. The temperature data at the nine probes were recorded by the acquisition system at every one minute, and were stored in a PC connected with the acquisition system (shown in Figure 3.19). Then the data files were transferred into an input file to be called by the model program in *Mathematica* and compared with the model predictions.

Figure 3. 19 Testing set up with the data acquisition system for automatically recording data at specified time step.

The 2D heat conduction model described above is for any two directions of any dimensions with known thermal conductivities in the specified directions. The radial and tangential thermal conductivities derived in the previous chapter are for the ideal situation as in the model simulation described above. The radial and tangential thermal conductivity values will be used only when there is perfect ring orientation as drawn in Figure 3.2. In the practical wood samples, the ring orientation is usually curved with different degrees deviated from the perfect orientation. Therefore in order to predict the temperature profiles in the two specified directions in the practical wood samples, modification on the true radial and tangential thermal conductivity values derived in the last chapter should be made to obtain the values in the two practical directions on wood blocks. Therefore the image of wood blocks' cross section need to be taken for measuring the latewood percentage and angles of the ring curve.

The cross section image of each wood block was taken by the camera and loaded into the image analysis software for the required measurements. Angles of the curved rings were measured at 10 random positions and averaged for the value to be used in the program. Latewood percentage was also measured by one of the tools in the image analysis software. Results are shown in the next section.

3.4.2 Results and Conclusions

3.4.2.1 Estimation of the practical thermal conductivities in the two transverse directions on wood blocks

Thermal conductivities in the two transverse directions on an actual wood sample are usually different from the true radial and tangential direction values as described in the theoretical models. Therefore the two practical thermal conductivities were calculated from the theoretical values by using the trigonometry and the technique of rotating the coordinates. An example of a practical wood sample with curved rings is shown in Figure 3.20.

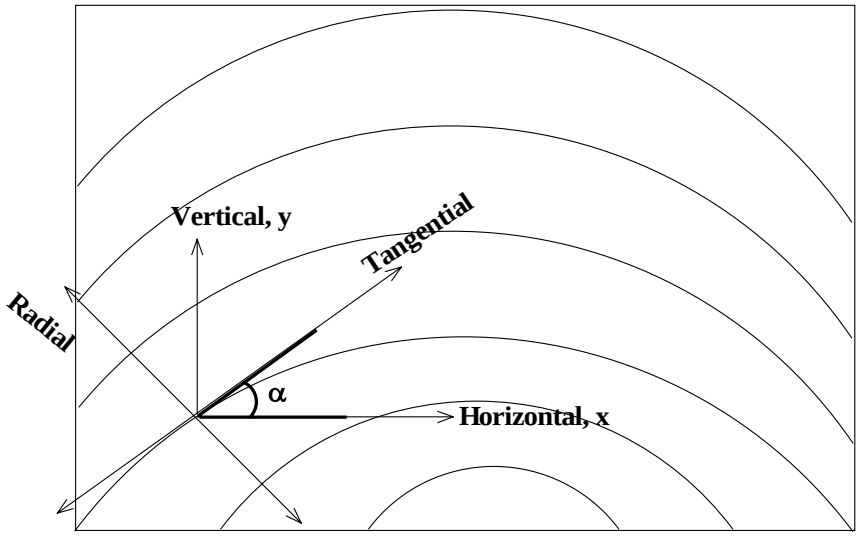

Figure 3. 20 A drawing of a practical wood sample's cross section with illustration of the four specified directions and the angle of the ring curves.

The two practical directions x and y shown in this figure are not exactly radial and tangential directions as defined by the wood anatomical structure. Therefore they will be called vertical and horizontal directions in the following. Thermal conductivities in these two directions can be calculated by rotating the radial-tangential coordinates onto the vertical-horizontal coordinates by using the angle for the rotation.

$$k_{vertical} = k_{radial} \cdot Cos\alpha + k_{\tan gential} \cdot Sin\alpha$$

Equa (3. 25)

$$k_{horizontal} = k_{radial} \cdot Sin\alpha + k_{\tan gential} \cdot Cos\alpha$$

Equa (3. 26)

Obviously the α angle is changed with the position. Therefore the practical thermal conductivity values are also changed with the location. However, in the program written for solving the 2D model, the thermal conductivities were assumed to be constant with the position. So one average angle from the measurements was taken for the calculation. The angle and latewood percentage for each testing block measured by the image analysis software was displayed in table 3.

Table 3. 1 Average results from the measurements for the angle and latewood percent on the cross section of each testing block.

Species	Latewood %	Angle (deg.)
Southern yellow pine	39%	35
scots pine	60%	50
maple	20%	25

The theoretical radial and tangential thermal conductivity values were obtained from the tables (table A-34 to table A-40 in the Appendix A) developed from the geometrical models in previous chapter based on the latewood percentage and moisture content measured from the testing samples. Then the table values were plugged in equation 3.22 and 3.23 to calculate the thermal conductivities in the two practical directions (vertical and horizontal). This step was edited into the program for easy repetition and modification.

The program may need to be revised in the future to include the position factor into the thermal conductivity functions.

3.4.2.2 Transient temperature from model predictions and testing results

Changes of temperature with time at nine points for each species were plotted in Figure 3.21 (southern yellow pine), 3.22 (Scots pine) and 3.23 (maple). They were plotted in two ways. One is along the vertical direction (red lines), the other is along the horizontal direction (green lines) for investigating the difference of the heat transfer in the two directions.

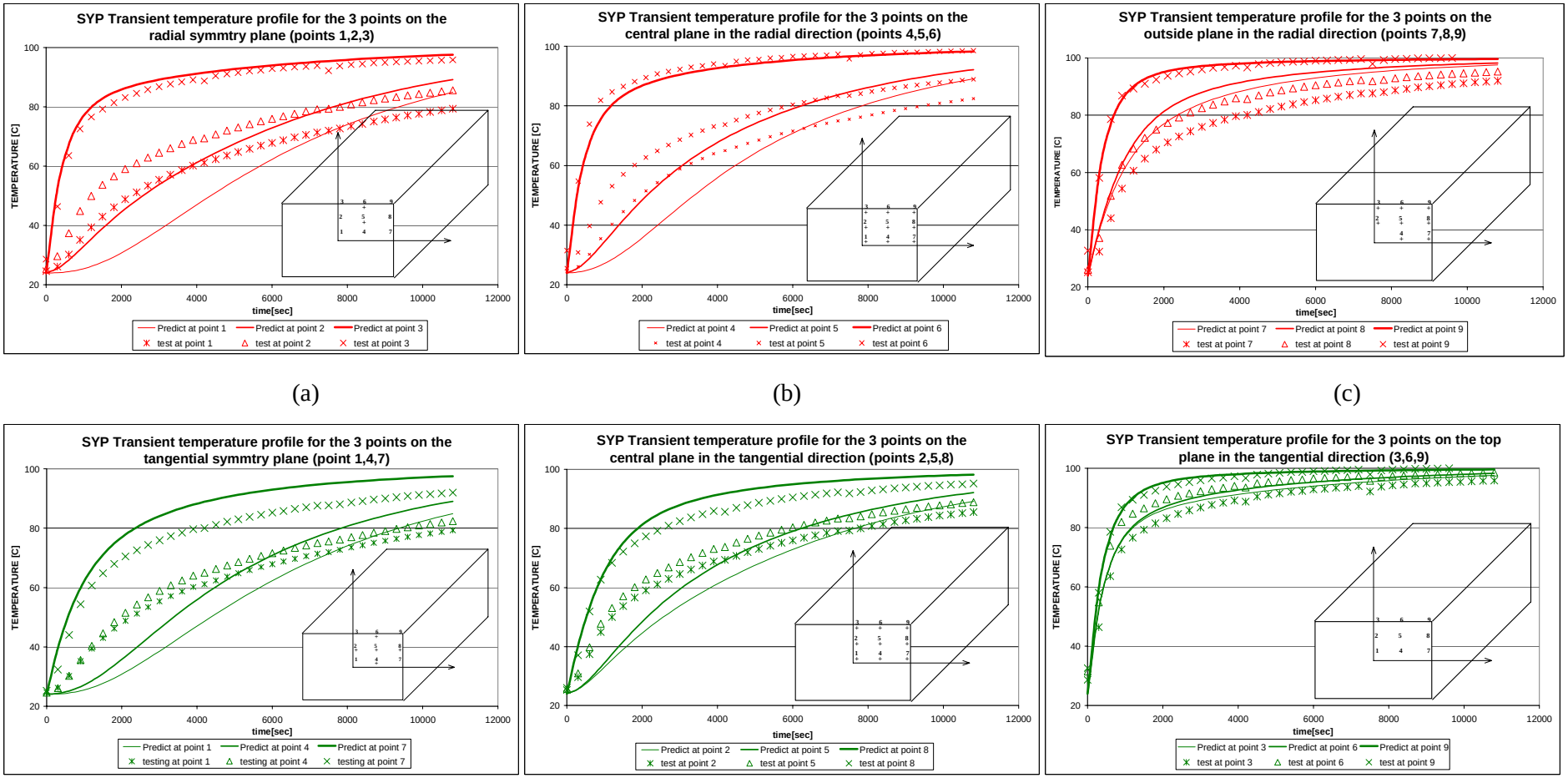

Figure 3. 21 Model prediction and testing results for the temperature profiles at the nine points on southern yellow pine wood block. (a),(b),(c) are for the vertical direction plot and (a'),(b'),(c') are for the horizontal direction plot.

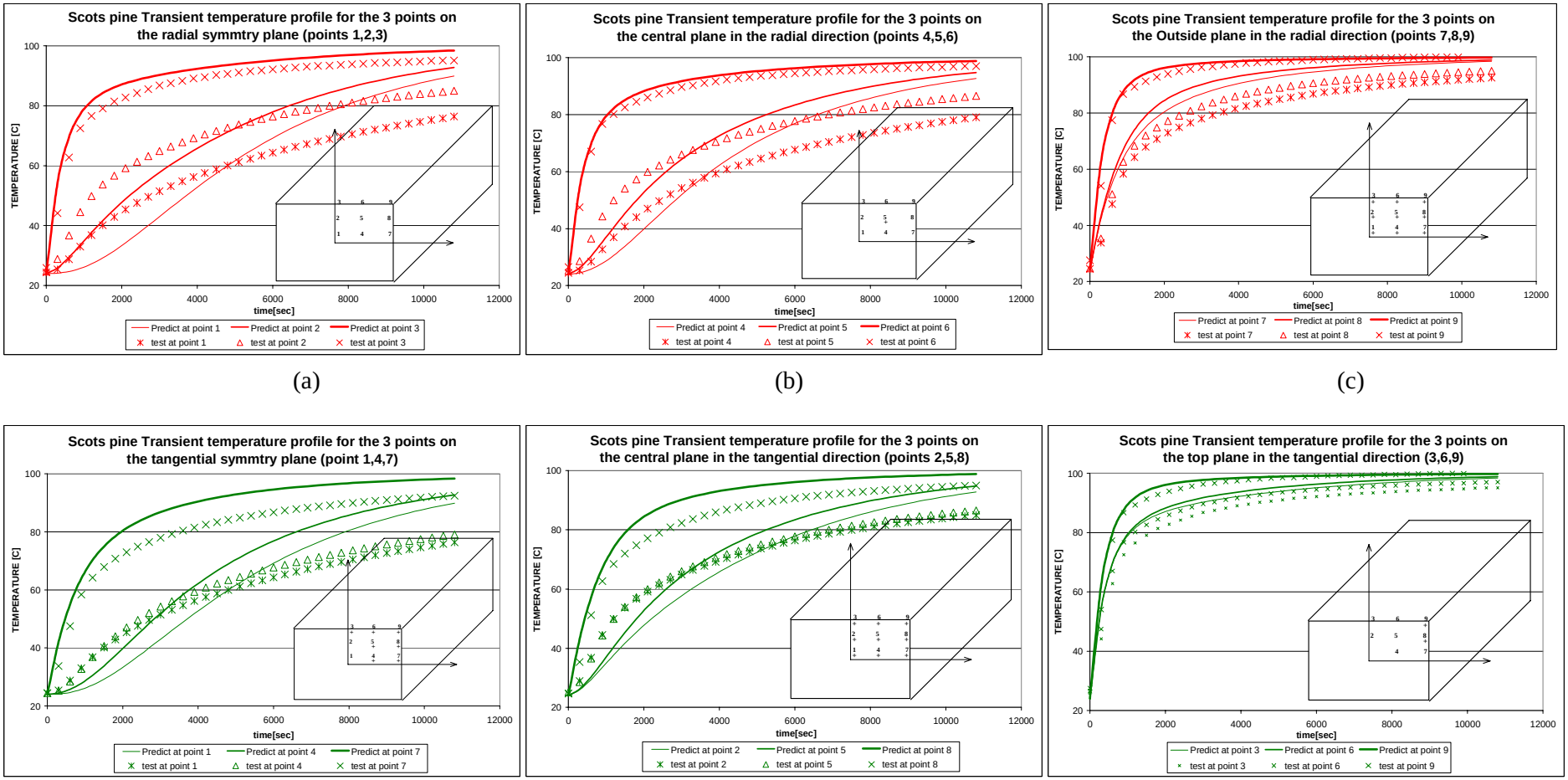

Figure 3. 22 Model prediction and testing results for the temperature profiles at the nine points on Scots pine wood block. (a),(b),(c) are for the vertical direction plot and (a'),(b'),(c') are for the horizontal direction plot.

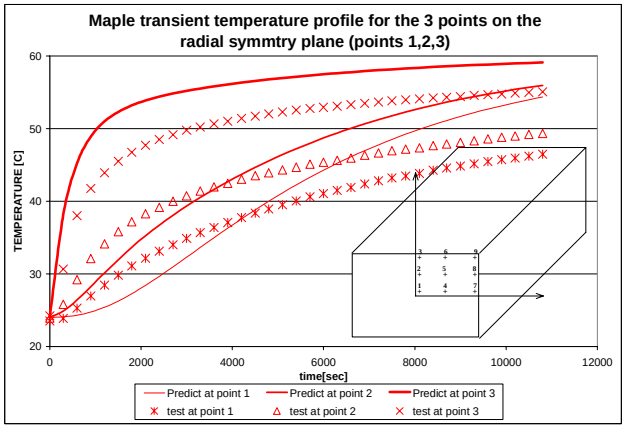

(a)

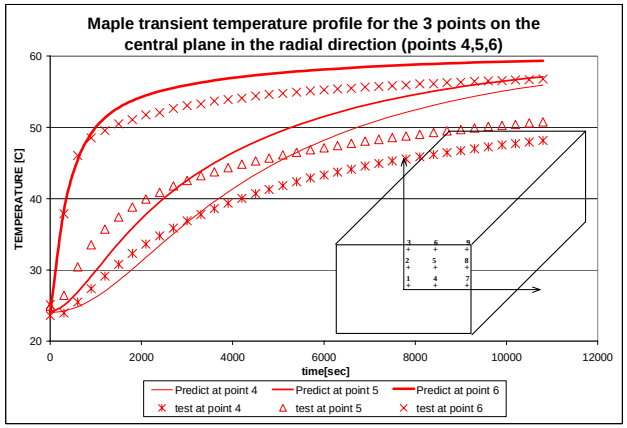

(b)

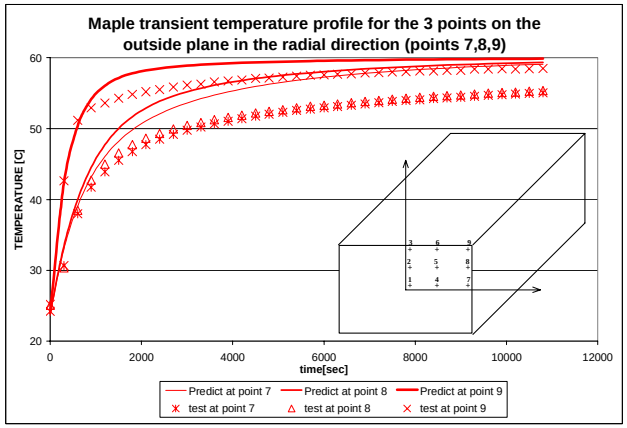

(c)

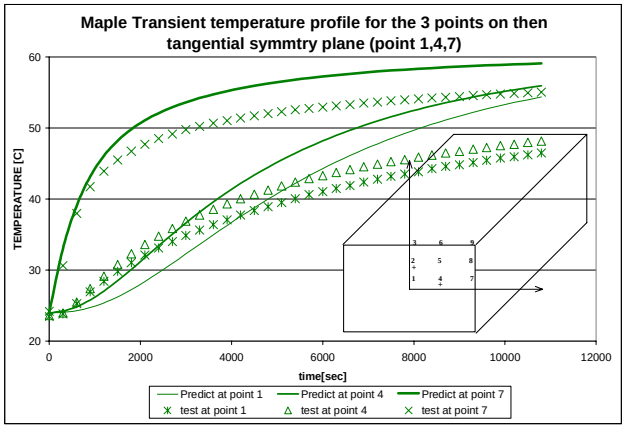

(a')

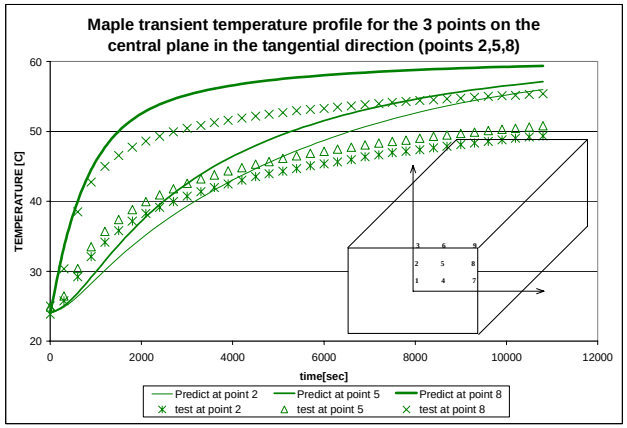

(b')

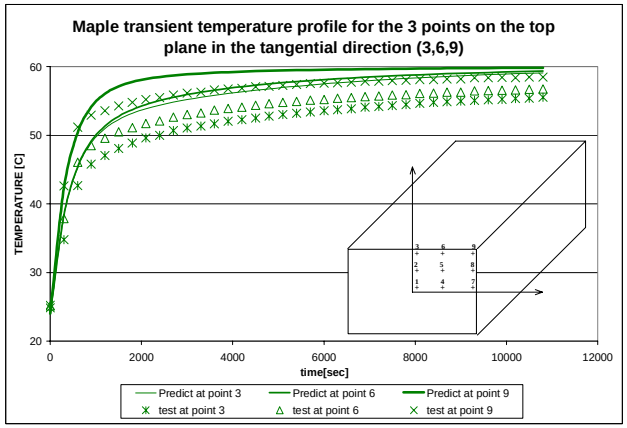

(c')

Figure 3. 23 Model prediction and testing results for the temperature profiles at the nine points on Soft maple wood block. (a),(b),(c) are for the vertical direction plot and (a'),(b'),(c') are for the horizontal direction plot.

The 2D model solved in this study gave a good prediction for the heat transfer in the two directions of wood blocks as shown in all the graphs. From the model predictions and testing results, it was shown that heat transfer in wood started with a fast increase at the beginning of the heating process, then followed with a slow rate of temperature increase until gradually reaching the boundary temperature. A little difference between the vertical plots and horizontal plots for all the three species can be found from the testing results. The temperatures near the surface (point 3 and 6) in the vertical plots (red graphs) are higher than the temperature (point 7,8) near the edge in the horizontal plots (green graphs) due to the little higher vertical thermal conductivity. (Point 3,6,7,8 and 9 are not exactly on the surface when measured by the thermocouples and predicted with the model, but 6 mm inside from all the surfaces, for the consideration of accuracy and convenience.) For the points inside the wood blocks, temperature difference between points in the horizontal direction is smaller than the temperature difference between the corresponding points in the vertical direction. For instance, difference between points 1 and 4 or 2 and 8 in the horizontal plots (graph (a'),(b') in all the three figures is smaller than the difference between points 1 and 2 or 4 and 5 (graph (a), (b)). Therefore the temperature increase near the center of wood has a higher slope in the vertical direction than in the horizontal direction. Model outputs (shown in the graphs) predict the same trends as the testing results. In general, the temperature change in the vertical and horizontal directions does not show significant difference due to the similar thermal conductivity values in the two directions obtained from the calculation by the true radial and tangential thermal conductivities.

The small discrepancy between the model predictions and testing results came from the moisture transfer effect on the heat transfer mechanism since the testing samples were not 0% moisture content. Heat and mass transfer are always coupled together and unseparated during the drying process. In this 2D heat conduction model, mass transfer was eliminated for the purpose of this study and mathematical simplification. The discrepancy may also come from the parameters used in the model, which were obtained either from literature or by an estimation. The model predicted higher temperatures for all the points near the surface and edge. This may be due to the higher convective coefficients used in the model ($h_{top}=6.92$, $h_{edge}=8.47$). The model predicted lower temperatures for the inside points (point 1,2,4,5) than the testing results at the beginning of heating, but predicted higher for these points than the testing results in the later heating process (time> 1 hour for Scots pine and maple, time>2 hours for southern yellow pine). This may be due to the constant specific heat value used in the model program. The specific heat (C_p) of wood has been tested by several studies as a function of temperature. In the model solved here it was

simplified as a constant value (2805 kJ/kg.K) obtained from the table A.3 in Incropera & DeWitt (1981). The specific heat of a substance is the amount of energy required to raise 1 gram of this substance 1°C. The product of density (ρ) and specific heat (C_p) is commonly used and termed the volumetric heat capacity (units of kJ/m^3.K). Heat capacity measures the ability of a material to store thermal energy. In the heat transfer analysis, the ratio of the thermal conductivity to the heat capacity is an important property termed the thermal diffusivity α with units of m^2/s :

$$\alpha = \frac{k}{\rho C_p}$$

Equa (3. 27)

It measures the ability of a material to conduct thermal energy relative to its ability to store thermal energy. Material of large α will respond quickly to the changes in their thermal environment, while material of small α will respond more slowly, taking longer to reach a new equilibrium condition. If the specific heat is estimated higher than its true value, as in the model for the beginning of the heat which has a relative low average temperature within the wood block, the thermal diffusivity α will be lower than its true value, and results in a slower modeled response to the changes of environmental temperature. Contrary to the early heating, average temperature in wood blocks became higher during the late heating period. The specific heat was also increased with the average temperature. Then the constant specified value used in the model program became lower than the true specific heat value, which resulted in higher thermal diffusivity than expected. Therefore the model predicted temperature at the inside of wood block responded more quickly to the changes of environment than the test measurements.

The thermal conductivity values used in the model gave good predictions for the model. The model predicted differences between the three temperature profiles in each graph match the three testing profiles well. This demonstrated that the heat transfer rate (thermal conductivity) in the spatial domain predicted well by the models developed in this study with the experimental results.

The results for the two softwood species were close and with a better fit than the hardwood species -- maple. This was due to the moisture content in maple wood block is much higher than the two softwood species, with a value of MC=35%. Therefore in the late heating process, temperature at all points on the block were measured lower than the model predicted. The moisture in wood needs energy for vaporization and movement. Only after the moisture

moves out of the sample, may temperature in wood increase to equilibrate with the boundary condition. Before the moisture moves out, the heat input into the wood sample was used for the moisture movement instead of increasing the temperature.

The 2D heat conduction model adequately predicted the major trends for the transient temperature profiles inside the wood blocks. The thermal conductivity values modified from the theoretical values (developed in last chapter) were also proven to be good estimations for the model parameters used in the program. The model output can be further improved by including the spatial factor into the thermal conductivity functions and including the temperature effect into the specific heat values used in the program. The external heat convective transfer coefficient is also an important factor for the model predictions, and it is very hard to measure practically.

3.4.3 Sensitivity study for the 2D heat conduction model.

As discussed above, the parameters used in the model may have different effects on the model predictions. Therefore sensitivity studies for the three parameters -- specific heat, thermal conductivity and convective heat coefficient -- were performed on southern yellow pine to investigate the relative importance of the model parameters.

Temperature changes with time at point 1,5,and 9 (displayed in Figure 3.9) were examined with response to the change of any one single parameter. Temperature sensitivity coefficient can be defined as (Zombori 2001):

$$X_T = \varphi \frac{\partial T}{\partial \varphi}$$

Equa (3. 28)

Where, φ ---- model parameter;

T ---- temperature;

The sensitivity coefficient indicates how sensitive the dependent variable (temperature) is to a small change of the specified parameter in the model. Observing the temperature sensitivity coefficients as functions of time provided insight for control of the heat transfer in wood.

The parameters -- specific heat C_p, thermal conductivity k, and heat convective coefficient h -- were either increased or decreased by 20% individually while leaving all the other parameters unchanged. The temperature sensitivity coefficient at the three points corresponding to the three parameters' change were plotted in Figure 3.24 , 3.25 , and 3.26 .

It is obvious that the temperature variable is not sensitive to the convective heat transfer coefficient at the boundaries. It has been discussed and shown in the simulation run for the southern yellow pine that the heat convective coefficient will only affect the inside temperature profile when there is a significant decrease in its values, such as one or two orders of magnitude decrease. Within the same order of magnitude or when h>1, no conceivable effect on the heat transfer in wood was found. This is due to the fast increase for the surface or edge temperature to equilibrate with the environmental temperature. So the thermal boundary layer disappeared quickly after the heating started. The inside temperature change will then depend on the heat

diffusion rate of wood. The non-significant effect from heat convective coefficient can also be explained by the Biot number, which is a dimensionless parameter measuring the temperature drop in the solid relative to the temperature difference between the surface and the boundary fluid. Biot number is defined as:

$$Bi = \frac{hL}{k}$$

Equa (3. 29)

When the ***Bi*** is very small (***Bi***<<1), which can be seen as $k>>h$ -- the conduction within the solid is much greater than the convection across the fluid boundary. Therefore the temperature transfer very fast inside the solid, and the solid has a pretty uniformly distributed temperature. When ***Bi*** ≈1, the conduction within the solid and the convection across the boundary are compatible. The ***Bi*** number calculated for the SYP simulation model was about 6~8. When keeping the L and k unchanged, and decreasing a 20% of h, ***Bi*** number decreases only by 20% with a value of 4~6. This small amount of ***Bi*** number change does not introduce any significant change on the inside heat transfer profile.

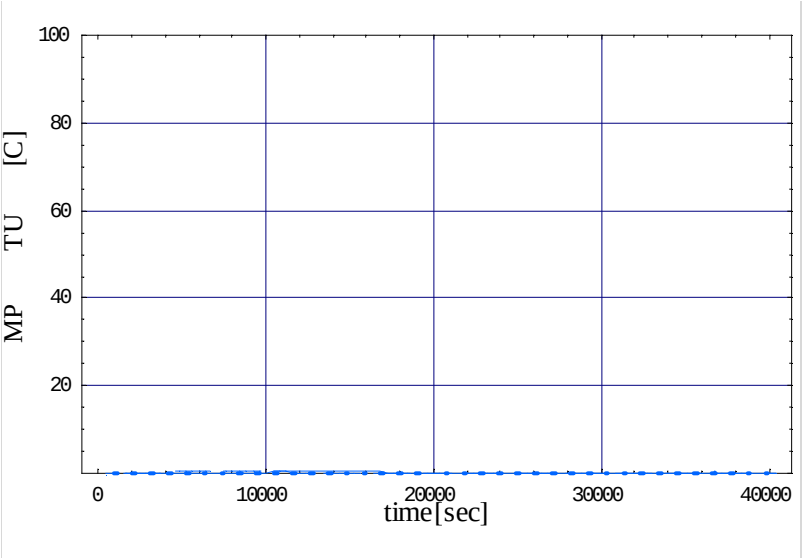

Figure 3. 24 Temperature sensitivity coefficient at the three points for the parameter of convective heat transfer coefficient (h_∞)at the boundary. (all the three point lines are very close the x axis).

It was shown in Figure 3.25 that the change of thermal conductivity had a significant effect on the transient temperature profiles predicted by the model. The temperature change increased with increase of thermal conductivity. The more inside the points are, the more significantly affected the temperature profiles are. But the time for the effect to start and reach the highest is different for the different points in wood blocks. It depends on the distance between the points and the external planes. As shown in the figure, the temperature changes at point 1 is much greater than the temperature change at point 9, but the temperature change with the change of thermal conductivity at point 9 is immediate when the heating starts. The other two inside points (1 and 5) increase gradually until reaching the top and then die off. This is due to the heat flow from outside to inside and when temperature is distributed uniformly within the wood block, the heat transfer became less and less. Therefore the thermal conductivity has less and less effect on the temperature profiles.

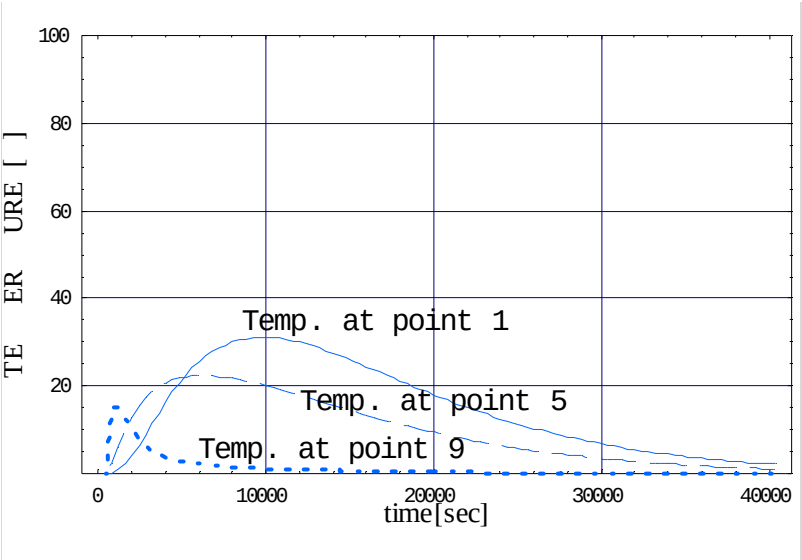

Figure 3. 25 Temperature sensitivity coefficients at the three points for the parameter of thermal conductivity (k_r and k_t) in wood.

The specific heat (C_p) had a similar trend of the effects as the thermal conductivity on the temperature profile changes within wood blocks. The difference between the two parameters is that they have the opposite effect on the temperature change. Transient temperature at all the points increased with the thermal conductivity increase, while the transient temperature in wood increased with the decrease of specific heat values. Figure 3.26 showed how the temperature

profiles responded to the 20% decrease of the specific heat value assumed in the model. The temperature responses to the specific heat change at the three points were similar to their response to the thermal conductivity change, but with the higher amount of increase for the temperature. The two similar effects from the thermal conductivity change and specific heat change can be explained by the thermal diffusivity α discussed before. The α is the ratio of thermal conductivity over the volumetric heat capacity (product of density with specific heat). It measures the ability of a material to conduct thermal energy relative to its ability to store thermal energy. If increasing the thermal conductivity of wood is increased, wood will conduct thermal energy faster, which resulted in an increase of temperature within the wood. On the contrary, if the specific heat is increased, wood will store more thermal energy. So the temperature will be lower. For both thermal conductivity and specific heat changes, the more interior the points are, the more affected the temperatures are at these points by the parameters' change.

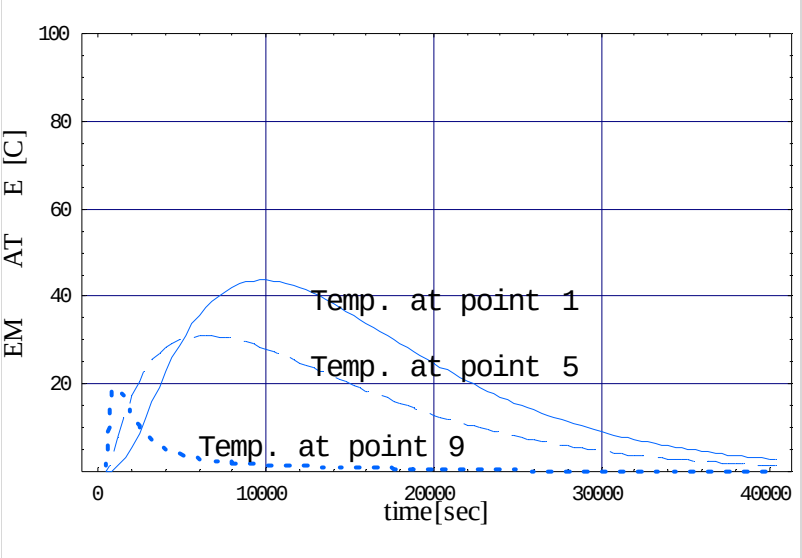

Figure 3. 26 Temperature sensitivity coefficient at the three points for the parameter of specific heat (C_p) in wood.

3.5 Conclusion

The two-dimensional heat conduction model was developed to utilize the theoretical values for the radial and tangential thermal conductivity derived from the previous chapter by the geometric model. The simulation run on a southern yellow pine block with an idealized anatomical structure showed the anisotropic material properties (thermal conductivity) effect on the heat transport in wood. Sharp increases of the temperature at the surface and edge boundaries were found right after the heating started due to the relative high heat convective coefficients. Heat transferred very fast during the early heating process, then slowed down to gradually reach the boundary temperature. Time series analysis was based on the 2D temperature plots at certain points with the time changing. Temperature at the very external point increased immediately to the environmental temperature, while the internal points' temperature increased gradually to the equilibrium. The temperature profiles at the three points along the radial direction were compared with the temperature profiles along the tangential direction. It was found that heat transferred a little faster in the radial direction than in the tangential direction due to the higher radial thermal conductivity values used in the model simulation. The external heat convective coefficient (h_∞) effect on the heat transportation was examined by running the program with three different assumed coefficient values. It was found that no significant effect on the heat transfer profiles from the heat convection coefficient (h_∞) when h_∞ is greater than 1 and less than 100, but there was a significant reduce for the heat transfer when h_∞ was reduced 2 order of magnitude (10^{-2}).This can be explained by the Biot number ($Bi= h_\infty L/k$). Spatial analysis was based on a series of temperature distribution at certain plane along radial or tangential direction plotted at several time steps. Temperature gradient was higher within the area near the surface and edge. The differential of the temperature was decreasing with time until the temperature equilibrium was reached within the block. Heat transfer faster in the radial direction than in the tangential direction but with tangential heat transfer catching up at the late heating stage.

Validation tests for the 2D heat conduction model were performed on the three species chosen for this study. Model outputs were based on modification of the thermal conductivity in the practical two transverse directions on wood blocks. The comparison of the model output with the testing results showed good predictions for the 2D model developed for heat conduction in wood. Heat transfer in the two practical transverse direction (vertical and horizontal direction) did not show significant differences due to the close thermal conductivity values in the two directions modified from the theoretical radial and tangential thermal conductivities. The parameters used in

the model were important factors. The sensitivity studies of the three parameters showed no significant effect of the external heat convection coefficients on the internal temperature change due to the relative high coefficients already used in the model predictions. Temperature change in the wood block was sensitive to both thermal conductivity and specific heat values change. They have the opposite effect on the temperature change based on the sensitivity study results and analysis from the thermal diffusivity (α) property of wood.

The 2D heat conduction model developed in this study can be further improved in the future by including the position factor into the thermal conductivity functions and adding a function for the specific heat with the changes of temperature in wood.

References:

Bonneau, P. and J.R. Puiggali. 1993. Influence of heartwood-sapwood proportions on the drying kinetics of a board. *Wood Science and Technology*, Vol.28:67-85.

Bories, S. 1986. Recent advances in modelisation of coupled heat and mass transfer in capillary-porous bodies. In: *Drying '89*, Eds. A.S. Mujumdar and M.A. Roques, Hemisphere Publ, N.Y.:46-62.

Bramhall, G. 1979. Mathematical model for lumber drying. I. Principles involved. *Wood Science*, Vol.12 (1):14-21.

Chen, P. and D.C.T. Pei. 1989. A mathematical model of drying processes. *International Journal of Heat Mass Transfer*, Vol.32(2):293-310.

Ferguson, W.J. and I.W. Turner. 1994. A two-dimensional numerical simulation of the dyring of pine at high temperatures. *Proc. 4th IUFRO Wood Drying Conference*, Rotorua, New Zealand: 415-422.

Haygreen, J.G. and J.L. Bowyer. 1982. Forest Products and Wood Science, An introduction. Iowa State University Press/Ames. 484pp.

Hearmon, R.F.S. and J.N. Burcham. 1955. Specific heat and heat of wetting of wood. Nature, Vol.176:978.

Hukka, A. 1997. Evaluation of parameter values for a high-temperatreu drying simulation model using direct drying experiments. *Drying Technology*, Vol.15(3&4):1213-1229.

Incropera, F.P. and D.P.DeWitt. 1981. Fundamentals of Heat and Mass Transfer. 4th Ed. School of Mechanical Engineering, Purdue University. John Willey & Sons, New York.

Kamke, F.A. and M.Vanek. 1992. Critical review of wood drying models: plan of study. *3rd IUFRO drying conference*, Vienna.

Kamke, F.A. and M. Vanek. 1994. Comparison of wood drying models. *4th IUFRO International Wood Drying Conference*, Rotorua, New Zealand.

Khattabi, A. and H.P. Steinhagen. 1994. Analysis of transient nonlinear heat conduction in wood using finite-difference solutions. *Holz als Roh- und Werkstoff*, Vol.52:272-278.

Khattabi, A. and H.P. Steinhagen. 1992. Numerical solution to two-dimensional heating of logs. *Holz als Roh- und Werkstoff*, Vol.50:308-312.

Liu, J., S. Avramidis, and S. Ellis. 1994. Simulation of heat and moisture transfer in wood during drying under constant ambient conditions. *Holzforschung*, Vol.48(3):236-240.

Luikov, A.V. 1975. Systems of differential equations of heat and mass transfer in capillary-porous bodies. *International Journal of Heat and Mass Transfer*, Vol.18:1-14.

Michel, D., M. Quintard, and J.R. Puiggali. 1987. Enperimental and numerical study of pine wood drying at low temperature. *In drying '87* : 185-194. ed. A.S. Mujumdar. Washington, D.C. Heimsphere.

Pang, S.S., T.A.G. Langrish, and R.D. Keey. 1994. Moisture movement in softwood timber at elevated temperatures. *Drying technology*, Vol.12(8):1897-1914.

Pang, S.S. 1996. Moisture content gradient in a softwood board during drying: simulation from a 2-D model and measurement. *Wood Science and Technology*, Vol.30:165-178.

Parrouffe and A.S. Mujumdar. 1988. Bibliography on mathematical models of drying and dryers. *Drying Technology*, Vol.6(2):305-330.

Perre, P. 1987. Measurements of softwoods' permeability to air: importance upon the dyring model. *International Journal of Heat and Mass Transfer*, Vol.14:519-529.

Perre, P., M. Moser, and M. Martin. 1993. Advances in transport phenomena during convective drying with superheated steam and moisture air. *International Journal of Heat and Mass Transfer*, Vol.36(11):2725-2746.

Perre, P., I.W. Turner, and J. Passard. 1999. 2-D Solution for drying with internal vaporization of anisotropic media. *AIChE Journal*, Vol.45(1):13-26.

Perre, P. and I.W. Turner. 1999. A 3-D version of TransPore: a comprehensive heat and mass transfer computational model for simulating the drying of porous media. *International Journal of Heat and Mass Transfer*, Vol.42:4501-4521.

Plumb, P.A., G.A. Spolek, and B.A. Olmstead. 1985. Heat and mass transfer in wood during drying. *International Journal of Heat and Mass Transfer*, Vol.28(9):1669-1678.

Puiggali, J.R. and M. Quintard. 1992. Properties and simplifying assumptions for classical drying models. *Advances in Drying*, Vol.5:109-143.

Quintard, M. and S. Whitaker., 1987. Ecoulement monophsique en milier poreux: effet des heterogeneities locales. *J. Mec. Theo. Appl.* Vol.6(5):691-726.

Quintard, M. and S. Whitaker., 1988. Two-phase flow in heterogeneous porous media: the method of large-scale averaging. *Transp. Porous Media*, Vol.3:357-413.

Ranta-Maunus, A. 1994. Computation of moisture transport and drying stresses by a 2-D FE-Programme. *In Proc. 4th IUFRO International wood drying conference*, New Zealand Forest Research Institute, Rotorua, New Zealand.

Rosen, H.N. 1980. Empirical model for characterizing wood drying curves. *Wood Science*, Vol.12(4):201-206.

Salin, J.G. 1990. Simulation of the timber drying process. Prediction of moisture and quality changes. Ph.D. Thesis. Abo Akademi, Filand.

Salin, J.G. 1991. Modeling of wood drying: a bibliography. *Drying technology*, Vol.9(3):775-793.

Siau, J.F. 1984. Transport Process in Wood. Springer Verlag, New York. 245p.

Skaar, C. 1988. Wood-water relations. Springer Verlag, New York. 279p.

Stamm, A.J. 1964. Wood and Cellulose Science. Ronald Press, New York., N.Y. 549p.

Stanish, M.A., G.S. Schajer, and F. Kayihan. 1986. A mathematical model of drying for hygroscopic porous media. *AIChE. J.*, Vol.32 (8):1301-1311.

Steinhagen, H.P. 1985. Computerized finite-difference method to calculate transient heat conduction with thawing. *Wood and Fiber Science*, Vol. 18(3):460-467.

Sutherland, J.W., I.W. Turner, and R.L. Northway. 1992. A theoretical and experimental investigation of the convective drying of Australian *Pinus radiata* timber. *Proc. 3rd IUFRO Wood Drying Conference*, Vienna, Austra.

Turner, I.W. 1996. A two-dimensional orthotropic model for simulating wood drying processes. *Appl. Math. Modeling*, Vol.20(1):60-81.

Vick, B. Fall 1999. Class hand-outs for ME 5304 -- Conduction Heat Transfer. Virginia Tech, Blacksburg, VA 24060.

Vogel, R. 1989. Modellierung des W□rme- und Stofftransportes und des mechanischen Spannungsfeldes bei der trocknung fester K∠rper am Beispiel der Schnittholztrocknung. Ph.D dissertation, Technische Universit□t Dresden, Germany. 149p.

Wood Handbook -- Wood as an Engineering Material, 1999. Printed by Forest Product Society. Forest Products Laboratory General Technical, USDA, Forest Products Laboratory. Madison, Wisconsin, U.S.A.

Zombori, B.G. 2001. Ph.D dissertation. Modeling the Transient Effects during the Hot-Presssing of Wood-Based Composites. Dept. of Wood Sci. & Forest Prods., Virginia Tech. Blacksburg, VA 24060. 212pp.